



JGR Biogeosciences

-

RESEARCH ARTICLE

10.1029/2023JG007839

Key Points:

- Evergreen forests began
 photosynthesis in spring ~3 weeks
 before end of snowmelt, deciduous
 forests ~4 weeks after end of snowmelt
- There is little evidence for lengthening of the photosynthetic season in the northern hemisphere forest flux tower record
- Interannual variation in onset and end of photosynthesis was related to air temperature

Supporting Information:

Supporting Information may be found in the online version of this article.

Correspondence to:

D. R. Bowling, david.bowling@utah.edu

Citation:

Bowling, D. R., Schädel, C., Smith, K. R., Richardson, A. D., Bahn, M., Arain, M. A., et al. (2024). Phenology of photosynthesis in winter-dormant temperate and boreal forests: Long-term observations from flux towers and quantitative evaluation of phenology models. *Journal of Geophysical Research: Biogeosciences*, 129, e2023JG007839. https://doi.org/10.1029/2023JG007839

Received 5 OCT 2023 Accepted 13 APR 2024

© 2024. The Authors.

This is an open access article under the terms of the Creative Commons

Attribution-NonCommercial-NoDerivs

License, which permits use and distribution in any medium, provided the original work is properly cited, the use is non-commercial and no modifications or adaptations are made.

Phenology of Photosynthesis in Winter-Dormant Temperate and Boreal Forests: Long-Term Observations From Flux Towers and Quantitative Evaluation of Phenology Models

David R. Bowling¹ D, Christina Schädel^{2,3}, Kenneth R. Smith¹ D, Andrew D. Richardson^{3,4} D, Michael Bahn⁵, M. Altaf Arain⁶ D, Andrej Varlagin⁷ D, Andrew P. Ouimette⁸, John M. Frank⁹, Alan G. Barr¹⁰, Ivan Mammarella¹¹ D, Ladislav Šigut¹² D, Vanessa Foord¹³ D, Sean P. Burns^{14,15} D, Leonardo Montagnani¹⁶ D, Marcy E. Litvak¹⁷ D, J. William Munger¹⁸ D, Hiroki Ikawa¹⁹, David Y. Hollinger⁸ D, Peter D. Blanken¹⁴ D, Masahito Ueyama²⁰ D, Giorgio Matteucci²¹, Christian Bernhofer²², Gil Bohrer²³ D, Hiroki Iwata²⁴ D, Andreas Ibrom²⁵, Kim Pilegaard²⁵, David L. Spittlehouse¹³, Hideki Kobayashi²⁶ D, Ankur R. Desai²⁷ D, Ralf M. Staebler²⁸ D, and T. Andrew Black²⁹

¹School of Biological Sciences, University of Utah, Salt Lake City, UT, USA, ²Woodwell Climate Research Center, Falmouth, MA, USA, ³Center for Ecosystem Science and Society, Northern Arizona University, Flagstaff, AZ, USA, ⁴School of Informatics, Computing, and Cyber Systems, Northern Arizona University, Flagstaff, AZ, USA, ⁵Institute of Ecology, University of Innsbruck, Innsbruck, Austria, ⁶School of Earth, Environment & Society, McMaster University, Hamilton, ON, Canada, ⁷A.N Severtsov Institute of Ecology and Evolution, Russian Academy of Sciences, Moscow, Russia, 8U. S. Department of Agriculture, Forest Service, Northern Research Station, Durham, NH, USA, 9U. S. Department of Agriculture, Forest Service, Rocky Mountain Research Station, Ft. Collins, CO, USA, ¹⁰Global Institute for Water Security, University of Saskatchewan, Saskatoon, SK, Canada, 11 Institute of Atmospheric and Earth System Research/Physics, Faculty of Science, University of Helsinki, Helsinki, Finland, ¹²Global Change Research Institute CAS, Brno, Czech Republic, ¹³British Columbia Ministry of Forests, Prince George, BC, Canada, ¹⁴Department of Geography, University of Colorado, Boulder, CO, USA, ¹⁵National Center for Atmospheric Research, Boulder, CO, USA, ¹⁶Faculty of Agricultural, Environmental and Food Sciences, Free University of Bolzano, Bolzano, Italy, ¹⁷Department of Biology, University of New Mexico, Albuquerque, NM, USA, ¹⁸Harvard University, Cambridge, MA, USA, ¹⁹Hokkaido Agricultural Research Center, National Agriculture and Food Research Organization, Hokkaido, Japan, ²⁰Graduate School of Agriculture, Osaka Metropolitan University, Osaka, Japan, ²¹National Research Council of Italy, Institute of BioEconomy, Sesto Fiorentino, Italy, ²²Chair of Meteorology, Institute of Hydrology and Meteorology, Faculty of Environmental Sciences, Technische Universität Dresden, Dresden, Germany, ²³Ohio State University, Columbus, OH, USA, ²⁴Department of Environmental Science, Shinshu University, Matsumoto, Japan, ²⁵Technical University of Denmark, Kgs. Lyngby, Denmark, ²⁶Research Institute for Global Change, Japan Agency for Marine-Earth Science and Technology, Yokosuka, Japan, ²⁷University of Wisconsin-Madison, Madison, WI, USA, ²⁸Air Quality Processes Section, Environment and Climate Change Canada, Gatineau, OC, Canada, 29 Faculty of Land & Food Systems, University of British Columbia, Vancouver, BC, Canada

Abstract We examined the seasonality of photosynthesis in 46 evergreen needleleaf (evergreen needleleaf forests (ENF)) and deciduous broadleaf (deciduous broadleaf forests (DBF)) forests across North America and Eurasia. We quantified the onset and end (Start_{GPP} and End_{GPP}) of photosynthesis in spring and autumn based on the response of net ecosystem exchange of CO2 to sunlight. To test the hypothesis that snowmelt is required for photosynthesis to begin, these were compared with end of snowmelt derived from soil temperature. ENF forests achieved 10% of summer photosynthetic capacity ~3 weeks before end of snowmelt, while DBF forests achieved that capacity ~4 weeks afterward. DBF forests increased photosynthetic capacity in spring faster (1.95% d⁻¹) than ENF (1.10% d⁻¹), and their active season length (End_{GPP}-Start_{GPP}) was ~50 days shorter. We hypothesized that warming has influenced timing of the photosynthesis season. We found minimal evidence for long-term change in Start_{GPP}, End_{GPP}, or air temperature, but their interannual anomalies were significantly correlated. Warmer weather was associated with earlier Start_{GPP} (1.3-2.5 days °C⁻¹) or later End_{GPP} (1.5-1.8 days °C⁻¹, depending on forest type and month). Finally, we tested whether existing phenological models could predict Start_{GPP} and End_{GPP}. For ENF forests, air temperature- and daylength-based models provided best predictions for Start_{GPP}, while a chilling-degree-day model was best for End_{GPP}. The root mean square errors (RMSE) between predicted and observed Start_{GPP} and End_{GPP} were 11.7 and 11.3 days, respectively. For DBF forests, temperature- and daylength-based models yielded the best results (RMSE 6.3 and 10.5 days).

Plain Language Summary We used records of forest-atmosphere carbon dioxide exchange and weather to determine when photosynthesis begins and ends each year in 46 northern hemisphere forests. We used observations of soil temperature to determine the timing of the end of the snowmelt period. We found that evergreen needleleaf forests began photosynthesis ~3 weeks before snowmelt ended, while deciduous broadleaf forests (DBF) waited until ~4 weeks after snowmelt ended. The DBF type ramped up photosynthesis in spring, and ramped down in autumn, faster than the ENF, and the length of the photosynthesis (or "growing") season was ~50 days shorter for DBF forests. Abundant evidence suggests that spring is occurring earlier in recent decades. We checked whether these forests are starting photosynthesis earlier by looking at forests with long-term records. We found minimal support for changes in photosynthetic phenology over time, but very strong connections between temperature and the timing of spring and autumn transitions. We tested 19 models that use weather data to predict plant phenological events. We used gridded weather data to drive the models, and the best models were able to predict the spring and autumn photosynthetic transitions to within ~10 days.

1. Introduction

Seasonally snow-covered forests of the northern temperate and boreal regions are an important component of the global carbon (C) cycle (Friedlingstein et al., 2022; Luyssaert et al., 2007). These forested regions span hundreds of millions of hectares (Brandt, 2009; Keenan et al., 2015), and contain substantial C reservoirs (Kurz et al., 2013). Currently they are a significant sink for C (Pan et al., 2011), but the future of that sink is highly uncertain (Friedlingstein et al., 2014) and reliant on forest response to environmental change.

The climate of northern latitudes is undergoing significant change (Gauthier et al., 2015). Temperature has risen markedly over the last few decades (Wang et al., 2019), bringing a host of associated changes. Temperature (T) strongly influences plant phenology, and plants have responded to warming with earlier leaf growth, flowering, and fruiting (Menzel et al., 2006). A global pattern of earlier spring onset and delayed autumn has been observed for deciduous plants (Garrity et al., 2011; Linderholm, 2006; Pilegaard & Ibrom, 2020; Schwartz et al., 2006; Vitasse et al., 2022; White et al., 2009). Satellite records of vegetation greenness indicate an extended photosynthetic season for deciduous forests across the northern hemisphere (Jeong et al., 2011; Myneni et al., 1997; Piao, Wang, Park, et al., 2020), and this has impacted land-atmosphere C exchange enough to alter the magnitude and timing of the seasonal cycle of atmospheric CO₂ (Barichivich et al., 2013; Piao, Wang, Park, et al., 2020). However, the impact of climate change on evergreen needleleaf forests (ENF) is less certain, as these forests maintain chlorophyll year-round and exhibit persistent greenness even during winter photosynthetic dormancy (Kong et al., 2020; Kunik et al., 2023; Magney et al., 2019; Walther et al., 2016).

Warming has also diminished the seasonal snow cover in North America (Mote et al., 2018; Siirila-Woodburn et al., 2021) and Europe (Beniston et al., 2018; Klein et al., 2016). Notable changes include reduced snow depth and snow water equivalent (SWE), increased rain/snow fraction, and earlier snowmelt, with potential feedback and additional warming through decreased albedo (Clare et al., 2023; Graf et al., 2023; McGuire et al., 2006). The onset of spring leaf flush in deciduous forests occurs after snowmelt (Black et al., 2000; Contosta et al., 2017), and changes in snowpack dynamics thus impact timing of photosynthesis. Satellite data reveal a long-term trend toward earlier snowmelt across large regions (Mioduszewski et al., 2015). Evidence suggests the timing of net C uptake by northern ecosystems and the onset of spring are now both earlier (Parazoo et al., 2018; Pulliainen et al., 2017). However, when forest cover is sparse, understory vegetation can dominate satellite observations of green up (Kobayashi et al., 2016).

Phenology and seasonal change in photosynthetic capacity dominate terrestrial gross primary productivity (GPP, Xia et al., 2015), and as such the implications of earlier spring onset for photosynthesis remain uncertain. The freeze-thaw transition provides a liquid water source to support transpiration, but only if the water transport pathway also thaws and remains so. Several studies have emphasized the significance of liquid water availability in the soil (e.g., Hollinger et al., 1999; Monson et al., 2005; Pierrat et al., 2021) and tree boles (Bowling et al., 2018; Nehemy et al., 2022; Sevanto et al., 2006) for spring initiation of GPP in ENF forests. If the soil and/or boles and stems are frozen, then liquid water cannot be transported through the xylem to support GPP, so one might expect that snowmelt would be an important event for photosynthesis to begin.

BOWLING ET AL. 2 of 25

Implications of earlier spring onset for annual carbon gain are also uncertain. In deciduous forests, a longer photosynthesis season often results in greater overall net C gain throughout the year (Finzi et al., 2020; Keenan et al., 2014), but higher spring uptake might lead to earlier senescence due to plant internal C sink limitation (Zani et al., 2020). Further, in regions with drier summers that rely on snowpack moisture during the photosynthesis season (Bailey et al., 2023; Goldsmith et al., 2022), earlier melt can lead to less C uptake over the year (Buermann et al., 2013; Hu et al., 2010; Knowles et al., 2018). The air T during the spring period also appears to be an important driver of spring C gain, as early melt combined with cold air and leaf T can limit photosynthesis during the melt period (Winchell et al., 2016). Colder soils due to decreasing snow can lead to delay of leaf flush (Desai et al., 2022). Other evidence suggests that warmer spring can lead to earlier senescence (Zohner et al., 2023). Warming experiments have shown that vulnerability to frost events in spring can lead to damage and mortality if the winter is not sufficiently cold to develop and maintain frost hardiness (Richardson et al., 2018).

There is currently no consensus among flux-tower based studies regarding long-term trends in the timing of photosynthesis. Trends toward earlier start and later end to the photosynthesis season have long been observed at large spatial scales using vegetation reflectance (Myneni et al., 1997; Piao, Wang, Park, et al., 2020; White et al., 2009), and microwave remote sensing has indicated widespread earlier thaw in the northern hemisphere, consistent with CO₂ fluxes in boreal forests (Pulliainen et al., 2017). The longer northern photosynthesis season has led to changes in the seasonality of atmospheric CO₂ (Piao, Wang, Park, et al., 2020). Despite these clear changes, conflicting analyses of long-term flux tower data indicate earlier (Keenan et al., 2014; Pilegaard & Ibrom, 2020; Xu et al., 2019) or no change (Wang et al., 2019) to the timing of the start of photosynthesis in spring. For deciduous species, the end of season has become later (Calinger & Curtis, 2023; Garrity et al., 2011; Pilegaard & Ibrom, 2020) or earlier (Hurdebise et al., 2019) in recent years. Moreover, recent reports highlight sub-annual lagged effects based on warming, wherein the previous summer's T influences spring photosynthetic timing (Gu et al., 2022), or increased early-season T leads to earlier senescence in autumn (Zohner et al., 2023). These changes are consistent with conceptual models of C fluxes hypothesized previously (Richardson et al., 2010).

Renewed interest in phenological responses to climate change has led to improved models to predict important phenological events for plants and animals (see reviews by Chuine & Régnière, 2017; Piao et al., 2019; Tang et al., 2016). These models can be grouped into categories based on a priori hypotheses about important environmental factors (see for example Post et al., 2022), such as air or soil T, accumulated T during spring warming or autumn chilling, daylength (photoperiod), and water availability. These "process-oriented" models are often parameterized to match observational data using optimization methods (Chuine et al., 1998, 1999), but inherent correlation among parameters may preclude physiological interpretation of model parameters. While phenological model parameters are often considered to be species-specific, the same models have also been used with good success when fit to multi-species stand-level phenological observations (Melaas et al., 2016). When calibrated to a sufficiently broad set of training data, even relatively simple phenological models with just a few parameters can make predictions that generalize well in time and space (Chen et al., 2016).

As Earth system models have added complexity and realism, it has become increasingly apparent that dynamic responses of the terrestrial biosphere to climate forcing must be faithfully represented (Chen, 2022; Song et al., 2021). Because the seasonality of many land-atmosphere feedbacks is regulated by phenology, enhancing phenological routines in these models is critical (Li et al., 2023; Peano et al., 2021; Richardson et al., 2012). For example, accurate representation of the seasonality of photosynthesis and evapotranspiration is a prerequisite for partitioning the surface energy budget (Barr et al., 2009), and for modeling soil moisture—both are critical to land-atmosphere coupling and feedbacks (Piao, Wang, Park, et al., 2020; Seneviratne et al., 2010). In a recent evaluation of the phenology schemes embedded in the Community Land Model (CLM versions 4.5 and 5.0), the modeled spring onset (change in leaf area index) was found to be much later than spring onset observed by MODIS in both temperate and boreal regions (Li et al., 2022); similar deficiencies have been reported for other land surface models (Peano et al., 2021).

In deciduous ecosystems, the primary challenge in phenological modeling involves accurately representing the seasonal dynamics of leaf area. This contrasts with temperate and boreal evergreen forests, where photosynthesis begins as trees emerge from winter dormancy (Bowling et al., 2018) but before new foliage grows in spring (e.g., Hollinger et al., 2021). Consequently, an alternative approach based on photosynthetic phenology is needed for evergreen forests. To ensure widespread applicability of phenological models, it is essential to understand the

BOWLING ET AL. 3 of 25

sensitivity of phenological events to environmental factors. This allows for extrapolation in time and space, enabling models to provide valid predictions about photosynthetic phenology and how it may respond to altered T and precipitation (Hänninen et al., 2018; Richardson et al., 2013).

In this study, we developed a new method to quantify the dates of the onset and end of photosynthesis, using the light response of net ecosystem exchange (NEE) of CO₂ (NEE). We compared these dates with estimates of the timing of end of snowmelt based on soil temperature to test: H1) Snowmelt is required for initiation of photosynthesis in winter-dormant forests in spring, and H2) Warmer temperature leads to earlier onset and later end to the photosynthesis season, at interannual and long-term time scales. Finally, to examine environmental influences on phenology of photosynthesis, and with the goal to improve phenological processes in terrestrial biosphere models (TBMs), we tested whether H3) existing phenological models can predict these phenological transitions when driven with gridded weather data.

2. Materials and Methods

2.1. Flux Tower Databases and Site Selection

Focusing on forests with cold season photosynthetic dormancy, we analyzed data from the AmeriFlux (ameriflux. lbl.gov), FLUXNET2015 (fluxnet.org), and Warm Winter 2020 (Warm Winter, 2020 Team, ICOS Ecosystem Thematic Center, 2022) databases. Initially, we considered all temperate and boreal forests in the northern hemisphere. We then selected sites with seasonal snow cover and winter photosynthetic dormancy based on (a) air T below freezing in winter, (b) high midday shortwave albedo in winter (where measured), (c) low short-term variation in soil T in winter (indicative of snow presence), (d) well-defined dormant periods in winter (identified by visual assessment of weekly mean NEE indicating no net C uptake), and (e) records of at least 3 years length. The R package *REddyProc* (version 1.3.2) was used to remove periods of low turbulence, with a site-specific friction velocity threshold (50 percentile), and to gap-fill NEE and weather data (Wutzler et al., 2018), but not for partitioning NEE into GPP and ecosystem respiration (see next section).

Our selection criteria led to a total of 46 flux towers for our analysis, consisting of 30 ENF, 14 deciduous broadleaf forests (DBF), and 2 mixed forests (sites are listed in Table S1 in Supporting Information S1). For analysis we combined the mixed and deciduous forests into a single group referred to as DBF. These study forests spanned a range of mean annual air T from -3.2 to 8.3° C, latitude from 35.9 to 67.4° N, and were located in North America and Eurasia. Overall, we analyzed a total of 578 site-years of data from these 46 forest sites. The period of record analyzed covered 1994–2021, and the distributions of representation of years analyzed are shown in Figure S1 in Supporting Information S1. Years analyzed for each forest site are shown in Table S1 in Supporting Information S1.

2.2. Flux Transition Dates Derived From NEE

We devised a novel method based on the light response of NEE to determine the seasonal dates marking the onset and end of the photosynthesis season. We deliberately avoided utilizing GPP derived from NEE flux partitioning. See Figure S2 in Supporting Information S1 and related discussion, and Section 3 of the SI for details on why a new approach was required.

Our method to determine seasonal transition dates from NEE and sunlight photosynthetically active radiation (PAR) is illustrated for a single site in Figure 1. We examined the light response of NEE (or lack thereof) from half-hourly (or hourly) data using a 5-day (5d) moving window. Representative examples are highlighted for a photosynthetically dormant period in winter and during the summer when photosynthesis is active (inset in Figure 1b). The mean NEE at night was taken to represent ecosystem respiration (R_{eco}) during each 5-day window, and the GPP light response was calculated by inverting the sign of NEE and removing the constant offset (inset in Figure 1c),

$$GPP = R_{eco} - NEE \tag{1}$$

where the sign convention for GPP and Reco are both positive, and NEE is negative during uptake (positive during release). This approach likely underestimates the magnitude of daytime respiration, particularly in the warm season. As a result, the associated estimates of GPP are also biased low relative to actual GPP. However, for

BOWLING ET AL. 4 of 25

21698961, 2024, 5, Downloaded from https://sgupubs.onlinelibrary.wiley.com/doi/10.1029/2023/G007839 by University Of Utah Spencer S, Wiley Online Library on [27.04.2024]. See the Terms and Conditions (https://onlinelibrary.wiley.com/terms-

and-conditions) on Wiley Online Library for rules of use; OA articles are governed by the applicable Creative Commons License

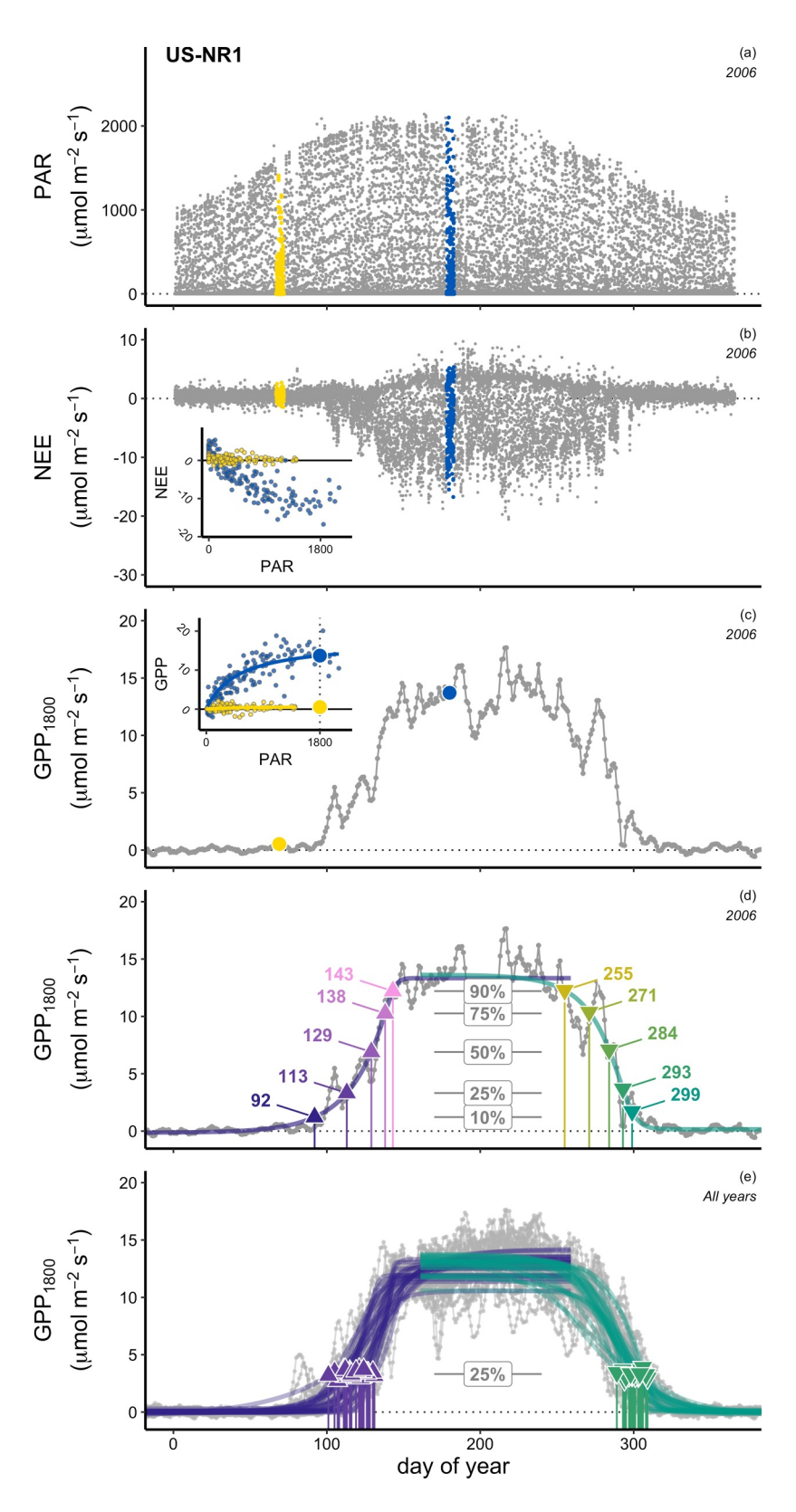


Figure 1.

BOWLING ET AL. 5 of 25



Journal of Geophysical Research: Biogeosciences

10.1029/2023JG007839

this study we are interested in the *timing* of seasonal change in the relation between light and photosynthesis, and the magnitude of GPP is unimportant.

We then applied a curve fit to the light response of the resulting GPP estimate:

$$GPP = \frac{a * PAR}{(1 + b * PAR)}$$
 (2)

where a and b are fit coefficients, and evaluated each 5d window at high light (PAR = 1,800 μ mol m⁻² s⁻¹). This value is arbitrary, but allowed us to examine seasonal change in the capacity for photosynthesis (Bowling et al., 2018). Initial analyses led us to fix the b coefficient to a constant value (0.002 m² s¹ μ mol⁻¹) which provided more robust results. In this way the shape of the light response curve is fixed and its saturation level is defined by a/b. We use the time series of GPP at high light (Figure 1c), which we refer to as $\mathbf{GPP_{1800}}$, to represent the annual pattern of whole-forest photosynthetic capacity, similar to a maximum photosynthesis rate (A_{max}) on a leaf-level photosynthetic light response curve.

The annual pattern of GPP_{1800} was used to determine transition dates that define the start and end of GPP ($Start_{GPP}$ and End_{GPP}) in spring and autumn, respectively. The annual pattern of GPP_{1800} (Figure 1c) was fit with two single logistic equations, one for the first part of the year and a separate one for the second part (Figure 1d). This approach allowed us to retain data for \sim half-years with long data gaps in spring or autumn. Details for the multi-step logistic fitting procedure are provided in the SI with Figure S3 in Supporting Information S1. Our approach differs from earlier usage of the double logistic equation by the flux community (Garrity et al., 2011; Gu et al., 2009; Yang & Noormets, 2021). From the logistic fits, we evaluated the percent distance from baseline to summer maximum (of fit line) at 5 thresholds that represent percentage of summer photosynthetic capacity (GPP_{1800}) present at a given time of year (10%, 25%, 50%, 75%, and 90%, Figure 1d). The use of multiple thresholds attempts to balance the tradeoff between ability to detect a transition and confidence that the result is robust (Richardson et al., 2009). Thus, for each site-year we calculated 5 variants for each of Start_{GPP} and End_{GPP} , one for each End_{GPP} threshold. The population of these dates for a End_{GPP} threshold of 25% for all years for Niwot Ridge (site US-NR1) is shown in Figure 1e.

The utility of open-path CO_2 analyzers has been identified as a challenge in cold conditions (Amiro, 2010; Burba et al., 2008; Wang et al., 2017), leading to potentially misleading conclusions about photosynthesis in winter. These analyzers are used by many in the flux tower community. However, we are interested in the *timing of transitions* between dormancy and photosynthesis, which are reliably detected despite this unavoidable issue.

2.3. Snow Cover Transition Dates Derived From Soil Temperature

A primary objective was to evaluate how the start and end of photosynthesis compared to the timing of dynamics of the snowpack (testing hypothesis H1). With few exceptions, our community has not installed sufficient instrumentation to monitor the snowpack at most flux towers, and site data to quantify snowpack properties such as cover, depth, or SWE were generally unavailable. We therefore used soil T to estimate when a snowpack was present. The soil thermodynamic environment under a snowpack is decoupled from energy exchange with the air and sky by the snow—this leads to fairly stable soil T with low variability in soil T even under shallow snow (Barr et al., 2009; Maurer & Bowling, 2014). We exploited the seasonal change in soil T variation to quantify when a snowpack was present (Groffman et al., 2001). For this, we used the shallowest soil T measurement available at

Figure 1. Illustration of the method for determining the timing of start and end of photosynthetic activity from the light response of net ecosystem exchange (NEE). Shown are the annual patterns of (a) photosynthetically active radiation (PAR) and (b) NEE for a single year. Selected 5-day periods are shown during the active season (blue) and the dormant season (yellow), and these are plotted as a light response of NEE (inset of panel b). The average NEE at night (PAR <5 μ mol m⁻² s⁻¹) was taken as an estimate of ecosystem respiration during each 5-day period to estimate the light response of gross primary productivity (GPP) (inset in panel c), and the value of GPP at high light (PAR = 1,800 μ mol m⁻² s⁻¹) was then calculated in similar fashion for all 5-day periods over the annual period (time series in panel c). This time series was fit using a single logistic curve for the first part of the year (purple), and a separate logistic function for the second part of the year (brown, details in Figure S3 in Supporting Information S1). Examples for a single year at site US-NR1 (Niwot Ridge) are shown in panel (d). Each curve was then divided into fractions from baseline to maximum, using 5 thresholds (10%, 25%, 50%, 75%, and 90%), and the day of occurrence for each threshold was assigned to the start of GPP (Start_{GPP}, dates on the rising edge (purple line) of the GPP₁₈₀₀ annual pattern), or end of GPP (End_{GPP}, dates on the falling edge, green line). Shown in panel (e) are all the dates for all years of record for this site at the 25% GPP₁₈₀₀ threshold, and the curve fits that they were derived from (purple and green lines).

BOWLING ET AL. 6 of 25

each site (closest to the soil/snow interface), which should have maximum diel variation at any time of year compared to greater depths.

The method is illustrated in Figure 2, with SWE and soil T shown for 1 year at Niwot Ridge (for validation, SWE in this case was measured by the USDA NRCS Snow Survey Program using a snow pillow \sim 400 m from the flux tower). The variation of soil T is low when there is snow present, contrasting markedly with the snow-free period, and the effect is consistent with even a minor amount of SWE (the inset in Figure 2e shows this pattern over many years). We fit the annual pattern of coefficient of variation (CV) of soil T using two single logistic equations as above (details in SI with Figure S4 in Supporting Information S1). From the fitted logistic equation, we determined the baseline and summer maximum of T variation (Figure 2d). The day of year by which a threshold of 10% of the variation range between the summer maximum and the threshold was first exceeded in the spring was determined as the end of the snowmelt period in spring ($\mathbf{End_{snow}}$) and when variation last dropped below that 10% threshold in the autumn was determined as the beginning of accumulation of snow in autumn ($\mathbf{Start_{snow}}$). The collection of $\mathbf{End_{snow}}$ and $\mathbf{Start_{snow}}$ dates for all years for Niwot Ridge is shown in Figure 2e. See Figures S5–S11 in Supporting Information S1 for validation of this method at sites where snow cover data were available.

We stress that **End**_{snow} indicates the end of the snowpack effect on soil T, and hence the end (not the start) of the melt period. Since this is based only on soil T it provides no direct information about liquid water associated with melt. Two sites were missing soil T data in the databases used and were omitted from snow-related analyses (US-Vcm, US-Pfa). The method failed to produce reliable estimates of Start_{snow} and End_{snow} for DK-Sor due to lack of clear seasonality in soil T.

2.4. Phenological Models

A major objective was to evaluate whether existing models of plant phenology could accurately predict the timing of the start and end of photosynthesis (Start_{GPP} and End_{GPP}) of temperate and boreal forests. We applied 19 spring and 3 autumn phenology models using the R package *phenor* (version 1.3.2), a modeling framework described by Hufkens et al. (2018). This package was developed to compare vegetation phenology data combined with location-specific gridded weather data obtained from the Daymet (Thornton et al., 2021) and E-OBS (Cornes et al., 2018) data sets for North America and Europe, respectively. The *phenor* package provides functions to quantitatively compare multiple models. Using pre-defined parameter ranges with a uniform distribution (non-informative Bayesian priors), we used simulated annealing to optimize parameters.

The phenology models are listed in Table 1 along with their drivers and number of parameters. The models represent different assumptions about the underlying environmental drivers and mechanisms controlling phenological transitions (none of the models include snowpack characteristics). The mathematical representation of these processes provides a wide range of model structures (for details, see Basler, 2016; Hufkens et al., 2018; Schädel et al., 2023) to be tested against the data. We used the principle of parsimony to guide model selection—the simplest model that can explain the observations is most useful. Akaike's Information Criterion (AIC) allowed us to balance complexity against goodness-of-fit.

The spring models ranged from a simple regression with air T to more complex nonlinear models including air T (warming and for some, chilling), photoperiod, and vapor pressure deficit, with 2–10 parameters depending on the model

For autumn models, we used three modifications of the chilling degree day (CDD) model (Table 1) in which leaf senescence occurs when the amount of chilling degree days is larger than a certain species-specific threshold (Jeong & Medvigy, 2014). The CDDP (chilling-degree day with photoperiod) model is adapted from the photo-thermal time (PTT) (spring thermal time with photoperiod) model and includes a photoperiod parameter (daylength in hours per day based on location) in the chilling requirement.

We used the function $pr_fm_phenocam$ to format flux data into a flattened nested list suitable for model comparison. All models were fit using the function pr_fit and parameter optimization was run using the GenSA generalized simulated annealing package in R (version 1.1.7, Xiang et al., 2013). The upper and lower limits for parameter ranges for all plant functional types (Table S2 in Supporting Information S1) were taken from Hufkens et al. (2018) and are within a biologically reasonable range. We ran the code on the high-performance computing cluster "Monsoon" (Northern Arizona University) in 25 parallel chains for each of the 40,000 iterations.

BOWLING ET AL. 7 of 25

21698961, 2024, 5, Downloaded from https://agupubs.onlinelibrary.wiley.com/doi/10.1029/2023JG007839 by University Of Utah Spencer S, Wiley Online Library on [27/04/2024]. See the Terms and Conditions (https://onlinelibrary.wiley.com/terms-

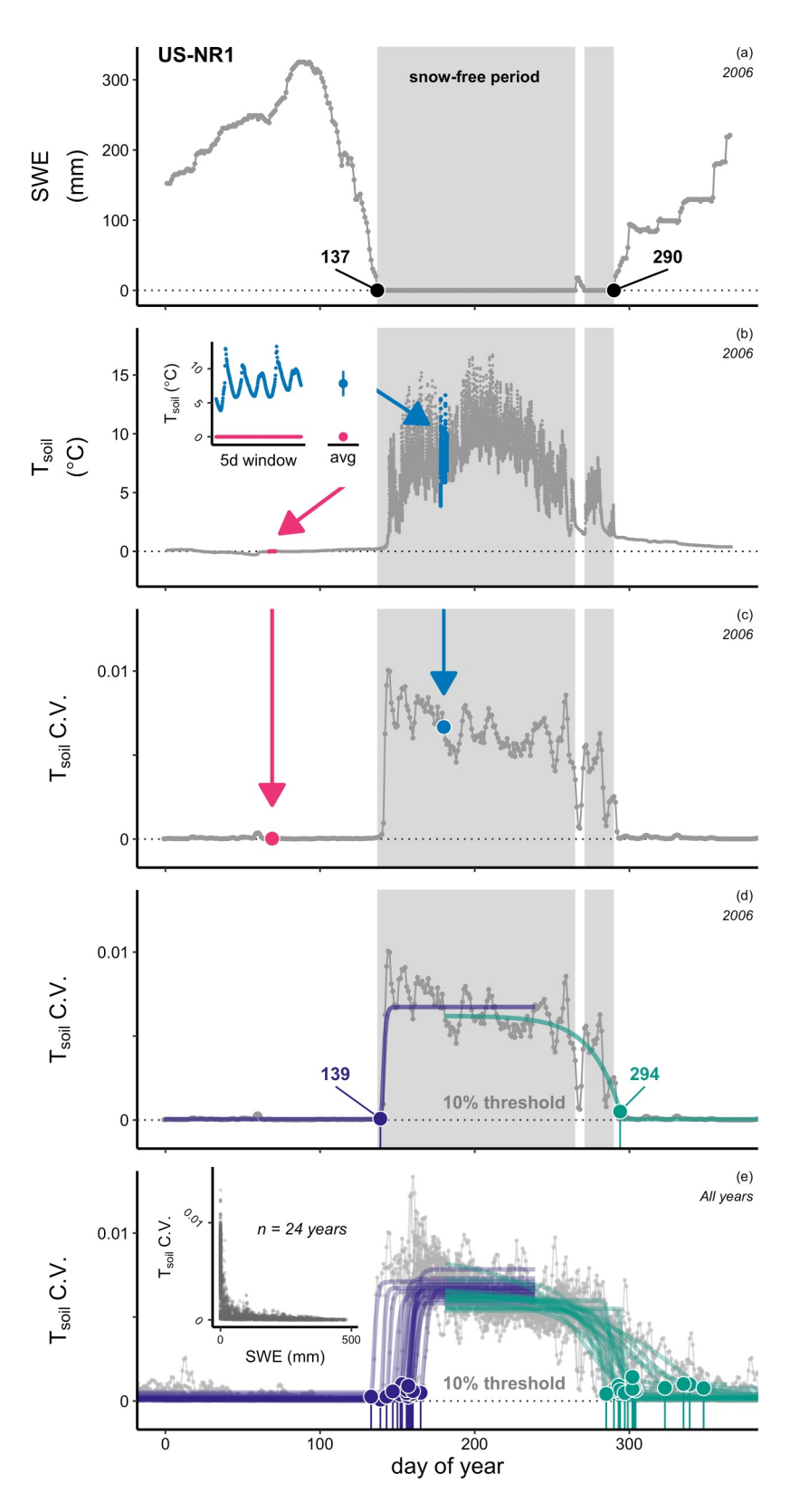


Figure 2.

BOWLING ET AL. 8 of 25

2.5. Statistical Analysis

We used two-way analysis of variance with forest type (ENF or DBF) and GPP_{1800} threshold as factors to (a) examine the timing of $Start_{GPP}$ in relation to end of snowmelt (testing hypothesis H1), and (b) compare the length of the photosynthetically-active season between forest types.

To evaluate whether there have been changes over time (years to decades) in the onset of GPP in spring or end of GPP in autumn (testing hypothesis H2), we evaluated site-level trends in observed $Start_{GPP}$ or End_{GPP} with time (year). For this we used sites with 10 or more years of data (28 forests total, 17 ENF and 11 DBF sites). The period of record for these longer flux tower data sets was 1994–2021, with most data density 2005–2015 (Figure S1 and Table S1 in Supporting Information S1).

We tested for significant changes three ways. First, we used simple linear regression (e.g., Start_{GPP} or End_{GPP} vs. year) and a Student's *t*-test to evaluate whether regression slopes were significantly different from zero. Second, we used the Mann-Kendall test via the *Kendall* package in R (version 2.2) to determine if there were significant trends. We tested all combinations of $Start_{GPP}$ and End_{GPP} with time, using all End_{GPP} thresholds. Regressions were performed on 280 total site-specific groups of dates ((17 ENF + 11 DBF sites) × 5 End_{GPP} or End_{GPP} with time (year), which is less sensitive to outliers than parametric linear regression (Sen, 1968). For this the R package *deming* (version 1.4) was used. Results are reported in Table 2 for those cases that were statistically significant. As a corollary to H2, we used simple linear regression to test for trends in monthly mean air T for sites with long records.

To evaluate (further testing H2) whether years with warmer spring or autumn are associated with earlier onset or later end to photosynthesis (or the reverse for cold years), we compared anomalies for $Start_{GPP}$ and End_{GPP} (at GPP_{1800} threshold of 10%) to anomalies of monthly mean air T for sites with records of 10+ years. Anomalies were computed related to the long-term mean for all years of record for each site independently. Data for ENF and DBF forests were grouped with all sites years in each forest type examined together. Simple linear regression was used to with a t-test for statistical significance as above.

The phenology models were evaluated in their ability to predict $Start_{GPP}$ and End_{GPP} (testing H3). The model output included model-predicted $Start_{GPP}$ and End_{GPP} , model parameter values, root mean square error (RMSE) from comparison of model predictions versus observed $Start_{GPP}$ and End_{GPP} , and AIC. To identify the best model for each season and forest type, we selected the model with the lowest AIC across all 25 parallel model runs for each season and functional type. We considered models with Δ AIC <2 to be equivalent in terms of performance, whereas models with Δ AIC \geq 2 had little support and models with Δ AIC \geq 10 no support (Burnham & Anderson, 2004).

2.6. Writing

The generative large-language model ChatGPT (https://openai.com/blog/chatgpt) was consulted to improve readability. This was used for language-related tasks, but not for creation or modification of scientific content, data, interpretation of results, or accession/interpretation of scientific literature.

Figure 2. Illustration of method for determining the timing of initial accumulation and end of melt of snowpack based on the coefficient of variation of soil temperature (T, at site US-NR1, 5 cm depth). Shown in panel (a) is a representative time series of snow water equivalent (SWE) (measured \sim 400 m from the tower), with the snow-free period indicated with shading, with the dates indicating the measured end of the melt period (day of year DOY 137) and the start of the next snowpack (DOY 290). Shown in panel (b) is the time series of soil T, with selected 5-day periods shown in the snow-free summer (blue) and in the snow-covered winter (red); the inset shows the soil T during each 5-day period (and the mean \pm 1 standard deviation). The coefficient of variation (CV) of soil T was calculated for each 5-day period during the year and is shown in panel (c), with the selected periods from panel (b) indicated in color (calculations made in Kelvins to avoid the sign of the Celsius scale). This time series was fit to a logistic curve for the first part of the year (purple line, d), and to a separate one for the second part (green line, details in Figure S4 in Supporting Information S1). A gray highlight marks the snow-free period, when the variation of T was above a threshold of 10% of the variation range between the summer maximum and baseline. The first and last exceedance of this threshold marked the end of the snowmelt period in spring (End_{snow}) and beginning of accumulation of snow in autumn (Start_{snow}, DOY 139 and 294, respectively, d). The collection of all years (n = 14) for this site, with corresponding dates, are shown in panel (e). The inset in panel (e) highlights the relation between measured SWE and the CV of soil T over these 24 years, demonstrating that even a shallow snowpack leads to minimal daily variation in soil T.

BOWLING ET AL. 9 of 25

Table 1

Details of Spring and Autumn Models Adapted From Basler (2016) and Hufkens et al. (2018)—See the Appendices of Those Papers for Full Model Descriptions

Model name	Abbreviation	Drivers	# Parameters	Reference/comments			
Spring							
Linear	LIN	F	2	Linear regression and temperature			
Thermal Time	TT	F	3	Cannell and Smith (1983), Hänninen (1990), Hunter and Lechowicz (1992)			
Thermal Time sigmoid	TTs	F	4				
*Photo-thermal time	PTT	PF	3	Črepinšek et al. (2006), Masle et al. (1989)			
Photo-thermal time sigmoid	PTTs	PF	4				
*M1	M1	PF	4	Blümel and Chmielewski (2012)			
*M1 sigmoid	M1s	PF	5				
Alternating	AT	CF	5	Cannell and Smith (1983), Murray et al. (1989)			
Sequential	SQ	CF	8	Hänninen (1990), Kramer (1994)			
Sequential b	SQb	CF	8				
*Sequential M1	SM1	CPF	9	Combination of Sequential and M1 model			
*Sequential M1b	SM1b	CPF	9				
Parallel	PA	CPF	9	Hänninen (1990), Kramer (1994), Landsberg (1974)			
Parallel b (bell-shaped)	PAb	CPF	9				
Parallel M1	PM1	CPF	10	Combination of Parallel and M1 model			
Parallel M1b (bell-shaped)	PM1b	CPF	10				
Unified M1	UM1	CPF	9	Chuine (2000)			
Growing season index	SGSI	FPV	9	Xin et al. (2015)			
Growing season index	AGSI	FPV	9	Xin et al. (2015)			
Autumn							
*Chilling degree day	CDD	C	3	Jeong and Medvigy (2014)			
Chilling degree day sigmoid	CDDs	C	4	Jeong and Medvigy (2014)			
*Chilling degree day photoperiod	CDDP	CP	3	Jeong and Medvigy (2014)			

Note. Models are grouped here by drivers: forcing temperature (F), chilling temperature (C), photoperiod/daylength (P), and vapor pressure deficit (V). Shading groups models with the same base structure together. Models with an asterisk were found to be optimal (see text).

3. Results

3.1. Timing of Seasonal Transitions

Transition dates between winter dormancy and active season GPP (Start_{GPP}, End_{GPP}) are shown for the 25% GPP₁₈₀₀ threshold and compared to snowpack dates (Start_{snow}, and End_{snow}) in Figure 3 (the transition dates for other thresholds may be found in Figures S12–S15 in Supporting Information S1). With one exception (CZ-BK1), GPP began at all sites after the spring equinox, and ended well after the autumn equinox (Figure 3). Interannual variability was apparent for all date types and all sites, with generally more variability in Start_{snow} and End_{snow} relative to Start_{GPP} or End_{GPP}. The standard deviations of multi-year anomalies of the snowpack dates relative to each site's mean date were ENF: 17.9 days in spring, 20.8 days in autumn, and DBF: 12.2 days in spring, 20.6 days in autumn, indicating that average year-to-year variation in snowpack melt or accumulation timing was a few weeks, with ranges in these site-specific timing anomalies as large as 50–60 days. Forests in warmer locations tended to have earlier start and later end to GPP (sites are ranked based on mean annual air temperature, MAT, in Figure 3), but there was much variation in this pattern. The DE-Hai (continental) and DK-Sor (near ocean) sites have similar MAT but likely different snowpack characteristics; we were not able to extract reasonable Start_{snow} or End_{snow} dates for DK-Sor.

BOWLING ET AL. 10 of 25

 Table 2

 Results of Regressions of Transition Dates Start_{GPP} and End_{GPP} Versus Time for Sites With 10 or More Years of Record

Database and site Bio		Date ne type	GPP _{sat} threshold (%)	n years	Linear regression				
	Biome				Slope (d yr ⁻¹)	Std error of slope (d yr ⁻¹)	<i>p</i> -value	Mann-Kendall trend p-value	Theil-Sen slope (d yr ⁻¹)
AMF_CA-LP1	ENF	Start _{GPP}	90	12	-2.19	1.17	0.09	0.05*	-1.95
AMF_CA-TP3			50	14	-1.30	0.65	0.07	0.02*	-1.40
AMF_US-Ha2			50	17	1.46	0.64	0.04*	0.12	1.40
AMF_US-Ho2			50	20	0.73	0.35	0.05*	0.07	0.80
AMF_US-NR1			90	23	0.74	0.34	0.04*	0.04*	0.92
WRM_CZ-BK1			90	11	3.78	1.14	0.01*	0.02*	3.25
WRM_FI-Let		25	10	3.49	1.05	0.01*	0.03*	4.17	
		50		2.86	0.47	0.00*	0.00*	2.57	
		75		1.70	0.67	0.03*	0.07	2.29	
AMF_US-Ha2 ENF	End_{GPP}	25	17	-1.07	0.56	0.08	0.03*	-1.21	
			50		-0.59	0.63	0.37	0.01*	-1.11
AMF_US-NR1		50	23	-0.46	0.20	0.03*	0.05*	-0.35	
		75		-0.74	0.30	0.02*	0.05*	-0.57	
			90		-0.99	0.45	0.04*	0.07	-0.71
AMF_US-Uaf			75	14	0.75	0.31	0.03*	0.01*	0.67
AMF_US-Vcm		25	10	-2.24	0.85	0.03*	0.01*	-2.60	
			50		-4.47	1.42	0.01*	0.01*	-4.14
			75		-5.45	1.94	0.02*	0.02*	-4.33
			90		-5.42	2.15	0.03*	0.05*	-3.00
WRM_IT-Ren		50	17	1.28	0.45	0.01*	0.04*	1.00	
			75		1.78	0.58	0.01*	0.01*	1.80
			90		1.87	0.82	0.04*	0.06	2.18
AMF_CA-Cbo DE	DBF	$Start_GPP$	10	24	0.67	0.26	0.02*	0.01*	0.69
			25		0.42	0.16	0.02*	0.06	0.38
FLX_IT-Col			10	12	-0.81	0.30	0.02*	0.02*	-0.65
			90		0.56	0.49	0.28	0.01*	0.69
AMF_US-Bar	DBF	End_{GPP}	10	14	1.20	0.43	0.02*	0.02*	1.20
AMF_US-Ha1			25	30	0.26	0.14	0.07*	0.01*	0.34
			50		0.23	0.17	0.17	0.01*	0.33
FLX_IT-Col			25	12	1.28	0.34	0.00*	0.02*	1.22
			50		1.76	0.66	0.02*	0.05*	1.50
FLX_US-PFa			75	18	-1.36	0.64	0.05*	0.06	-1.14

Note. Regressions with significant ($p \le 0.05$) linear regression slopes or Mann-Kendall trends are shown here (and bolded, they were not always significant together). Negative slopes imply a trend with transition dates occurring earlier in time (earlier $Start_{GPP}$ in spring or End_{GPP} in autumn in the later years of record), and positive slopes the reverse (later $Start_{GPP}$ or End_{GPP}). Database codes End_{GPP} 0 and End_{GPP} 1. Database codes End_{GPP} 2. Database codes End_{GPP} 3. Database codes End_{GPP} 4. Database codes End_{GPP} 5. Database codes End_{GPP} 6. Database codes End_{GPP} 8. Database codes End_{GPP} 9. Database codes End_{GPP} 9.

Evergreen needleleaf forests achieved 10% of their summer photosynthetic capacity about 3 weeks prior to the timing of full snowmelt (Figure 4e, the mean time when GPP $_{1800}$ reached 10% threshold was 17.7 days prior to the mean snowmelt date in ENF). In contrast, deciduous forests reached 10% capacity roughly 4 weeks after snowmelt (Figure 4e, mean for DBF 28.6 days). The GPP in ENF forests reached 50% capacity 19.4 days after snowmelt, and the DBF forests 54.4 days after snowmelt (Figure 4c). The mean increase from 10% to 90% of summer photosynthetic capacity took 73 and 41 days for ENF and DBF forests, respectively (comparing means

BOWLING ET AL. 11 of 25

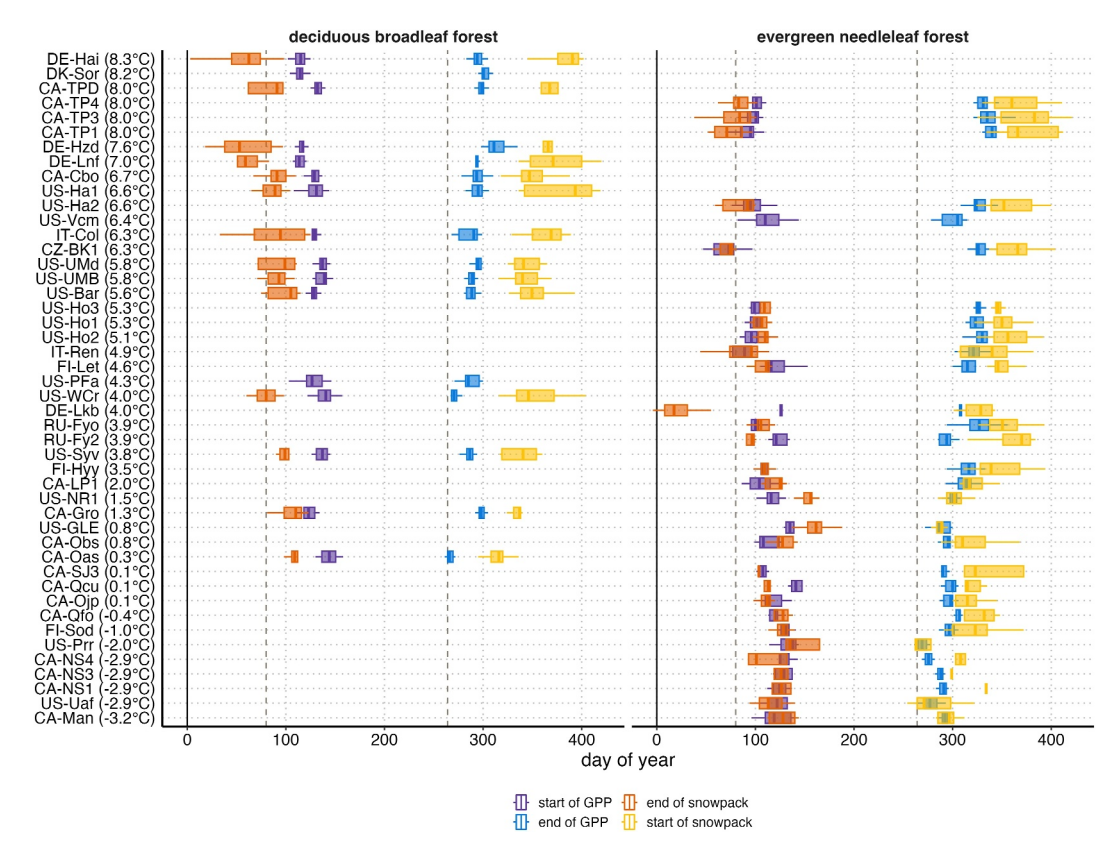


Figure 3. Boxplots highlighting the distribution of interannual variation in transition dates for each site, with sites ordered based on mean annual temperature (MAT in parentheses for each site, shown separately based on forest type (left and right panels). These are shown on the figure as Start_{GPP} (start of gross primary productivity (GPP), purple) and End_{GPP} (end of GPP, blue), and the start and end of snowpack accumulation and melt (Start_{snow} and End_{snow}, yellow and red, respectively). Vertical dashed lines indicate the spring and autumn equinoxes for comparison. Dates for GPP are shown for the 25% GPP₁₈₀₀ threshold; other thresholds can be examined in Supplemental Figures S12–S15 in Supporting Information S1.

for each forest type in Figures 4a and 4e). These data show an average rate of increase of photosynthetic capacity in spring of 1.10% and 1.95% d⁻¹ for ENF and DBF forests.

The length of the photosynthetically active season (End_{GPP}–Start_{GPP}) was longer for ENF compared to DBF by 49 days, when 10% GPP₁₈₀₀ thresholds were compared (Figure 4j), but only 10 days longer when 90% thresholds were compared (Figure 4f). This difference results from the length of time for each forest type to ramp up (and down) photosynthetic capacity in spring (autumn, Figure 4).

3.2. Evaluation of Long-Term Trends in Timing of Seasonal Transitions

We examined the time series of Start_{GPP} and End_{GPP} at sites with long records (10 or more years) to determine if there were trends such as earlier onset of photosynthesis in spring or later end in autumn. Results mostly showed no trends, those with trends were mixed and are shown in Table 2. In total, 280 regressions were examined for trends in Start_{GPP} and End_{GPP} with time (see Section 2). Only 32 regressions were significant (89% of regressions showed no trend).

Significant trends with time were found for 10 out of 17 evergreen forests and 5 out of 11 deciduous forests, in some cases for more than one GPP_{1800} threshold. Of the significant trends, spring initiation of GPP is occurring earlier (by 1.3–2.2 days yr^{-1}) in 2 ENF forests (CA-LP1 and CA-TP3), later in five others (US-Ha2, US-Ho2, US-NR1, CZ-BK1, and FI-Let) by 0.7–4.2 days yr^{-1} . and not changing in seven other forests. Patterns in autumn were also mixed with 3 forests showing earlier end to GPP, and 2 forests later end (Table 2). Only 2 deciduous forests showed significant trends in spring (CA-Cbo and IT-Col). Autumn end of GPP in deciduous forests is happening later at US-Bar, US-Ha1, and IT-Col, and earlier at US-PFa. Pilegaard and Ibrom (2020)

BOWLING ET AL. 12 of 25

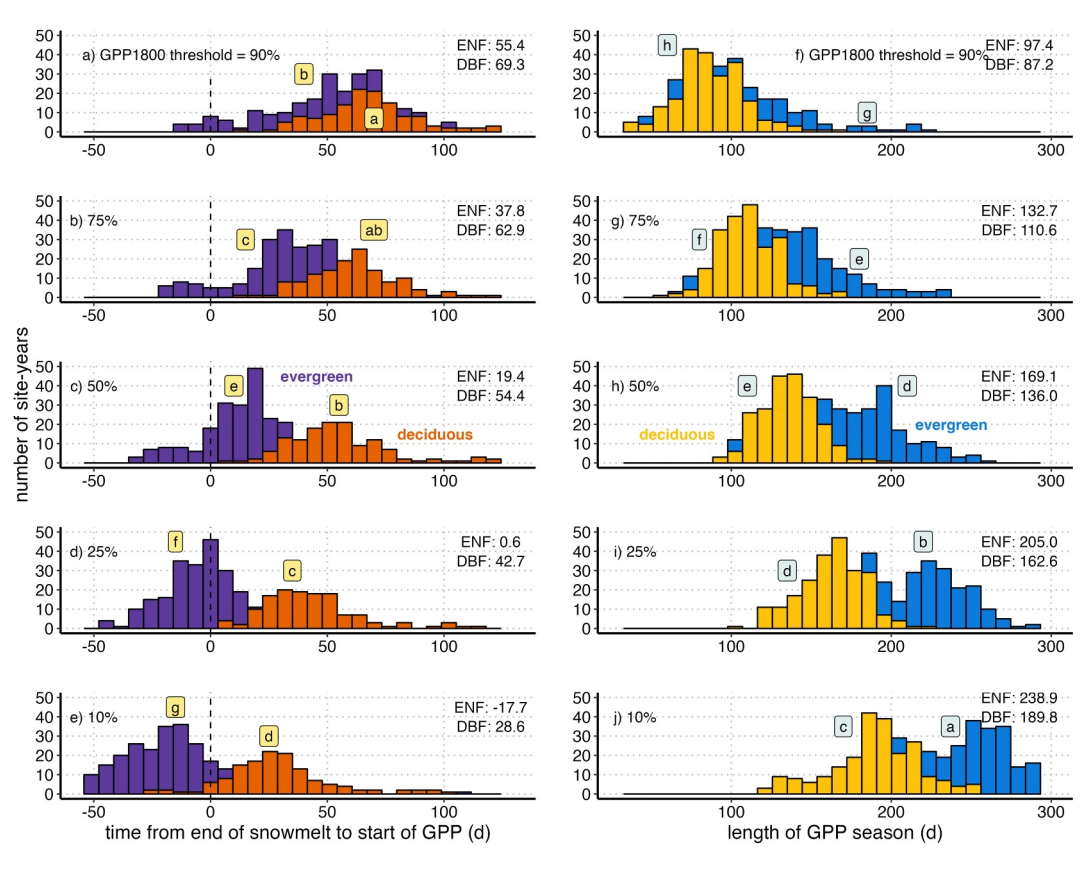


Figure 4. Left column: Frequency distributions of the difference (End_{snow}–Start_{GPP}) between end of snowmelt dates (calculated as in Figure 2) and start of gross primary productivity (GPP) in spring (as in Figure 1) for each of the GPP₁₈₀₀ thresholds (panels a–e). Negative values on horizontal axis indicate that GPP began before end of snowmelt, positive indicate that GPP began after end of snowmelt. Right column: Frequency distributions of the length of the GPP season (End_{GPP}–Start_{GPP}) for each GPP₁₈₀₀ threshold (panels f–j). Results are grouped for all evergreen and deciduous forests separately. Means for each distribution are shown in text on the right side of each panel. Letters indicate significantly different means between groups following two-way ANOVA, performed separately on the left and right columns.

found significant trends in both onset and end of photosynthesis at DK-Sor, which contrasts with our results using their data (no trend, Table 2). Our method requires PAR data which were missing or had long gaps in some years. Removing those years from the dates of the DK-Sor analysis of Pilegaard and Ibrom (2020) led to non-significant trends (data not shown).

To determine if the length of the photosynthetic season has changed over time, one should reasonably compare dates retrieved from the same GPP₁₈₀₀ thresholds in spring and autumn. The thresholds associated with significant trends differed across sites and from spring to autumn (Table 2). Significant trends were found at the same threshold in both spring and autumn at only two sites, (US-Ha2, US-NR1) with spring transitions later and fall transitions earlier, indicating a trend toward shorter photosynthesis season. For sites with changes in only spring or autumn (as noted above), the photosynthetic season is a bit longer (ENF: CA-LP1, CA-TP3, US-Uaf, IT-Ren, DBF: US-Bar, US-Ha1, US-PFa), or shorter (ENF: US-Ho2, CZ-BK1, FI-Let, US-Vcm, DBF: CA-Cbo) due to trends in the spring and fall dates as shown in Table 2.

Long-term trends in monthly mean air T at sites with long records are shown in Figure S17 in Supporting Information S1 (regressions of monthly mean T versus year for sites with records of 10+ years). Most sites and months showed no significant trend, and this was true whether the full record was used, or just those years represented in our analysis (years where $Start_{GPP}$ and End_{GPP} were available). Those that were significant indicate warming during those months ($<0.3^{\circ}C/yr^{-1}$), with a few exceptions that show cooling.

Anomalies of Start_{GPP} and End_{GPP} are compared with anomalies of air T in Figure 5 for March and September (other months are shown in Table S4 in Supporting Information S1). Across all forests in each type, regressions

BOWLING ET AL. 13 of 25

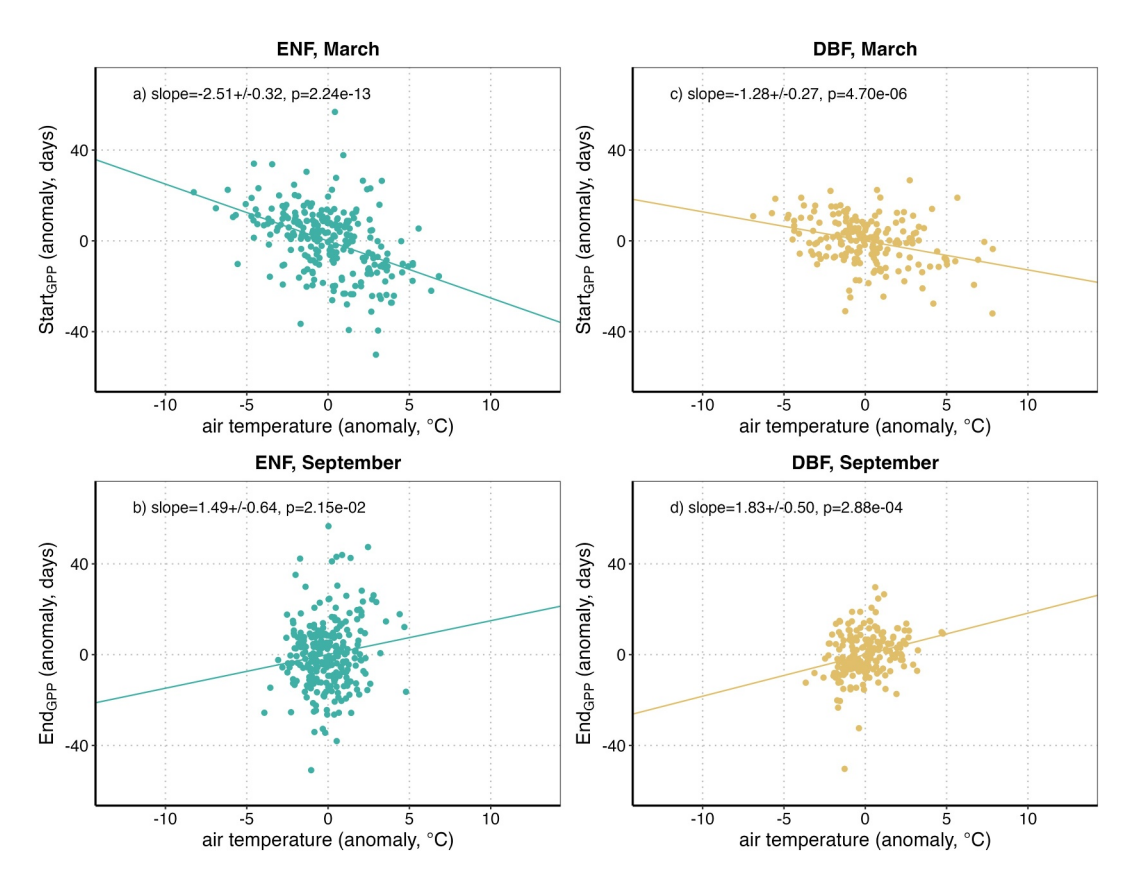


Figure 5. Anomalies of Start_{GPP} (top) and End_{GPP} (bottom, both at GPP₁₈₀₀ threshold of 10%) with monthly air T for evergreen needleleaf forests (a, b) and deciduous broadleaf forests (c, d), for the months of March and September. Regressions for other months can be found in Table S4 in Supporting Information S1.

were highly significant in these months. For both forest types, warmer spring was associated with earlier onset of photosynthesis (by 1.3-2.5 days ${}^{\circ}C^{-1}$), and warmer autumn with later end (1.5-1.8 days ${}^{\circ}C^{-1})$.

3.3. Phenology Model Predictions of Seasonal Transitions

The phenology models were most successful at predicting the $Start_{GPP}$ and End_{GPP} using the 25% GPP_{1800} threshold, except for DBF and $Start_{GPP}$ in which model predictions were best at 50% threshold (Figure S16 in Supporting Information S1, GPP_{1800} threshold with lowest RMSE group in each case). Plots of AIC showed the same pattern (not shown), with lowest AIC coinciding with the 25% threshold for ENF $Start_{GPP}$ and End_{GPP} , 25% End_{GPP} , and 50% End_{GPP} .

The best models in each case were chosen based on AIC (Figure 6, details of these models are provided in the Discussion, and optimized parameters for all models in Table S3 in Supporting Information S1). For evergreen forests, 4 models performed well for ENF in spring (Figure 6a); the best models were M1 (lowest AIC), PTT (Δ AIC from m1 = 0.15), and a combination of sequential and M1 models, SM1b (1.82), and SM1 (1.95). The best model for ENF forests in autumn was the CDD model (Figure 6b). In spring for DBF forests, the best predictions came from the M1s (lowest AIC) and M1 models (Δ AIC from m1s = 0.06, Figure 6c). The best model for DBF forests in autumn was the CDDP model (Figure 6d).

Predictions of Start_{GPP} and End_{GPP} from the best models are compared with the measured values in Figure 7. For evergreen forests, the M1 and CDD models predicted $Start_{GPP}$ and $Start_{GPP}$ with RMSE of 11.7 and 11.3 days (331 and 349 site-years of data, respectively, Figures 7a and 7b). For deciduous forests, the M1s and CDDP model predictions were slightly better, RMSE = 6.3 and 10.5 days (226 and 229 site-years, Figures 7c and 7d).

BOWLING ET AL. 14 of 25

21698961, 2024, 5, Downloaded from https://agupubs.

.com/doi/10.1029/2023JG007839 by University Of Utah Spencer S, Wiley Online Library on [27/04/2024]. See the Terms and Conditions (https://doi.org/10.1029/2023JG007839 by University Of Utah Spencer S, Wiley Online Library on [27/04/2024]. See the Terms and Conditions (https://doi.org/10.1029/2023JG007839 by University Of Utah Spencer S, Wiley Online Library on [27/04/2024]. See the Terms and Conditions (https://doi.org/10.1029/2023JG007839 by University Of Utah Spencer S, Wiley Online Library on [27/04/2024]. See the Terms and Conditions (https://doi.org/10.1029/2023JG007839 by University Of Utah Spencer S, Wiley Online Library on [27/04/2024]. See the Terms and Conditions (https://doi.org/10.1029/2023JG007839 by University Of Utah Spencer S, Wiley Online Library on [27/04/2024]. See the Terms and Conditions (https://doi.org/10.1029/2023JG007839 by University Of Utah Spencer S, Wiley Online Library on [27/04/2024]. See the Terms and Conditions (https://doi.org/10.1029/2023JG007839 by University Of Utah Spencer S, Wiley Online Library on [27/04/2024]. See the Terms and Conditions (https://doi.org/10.1029/2023JG007839 by University Order S, Wiley Online Library on [27/04/2024].

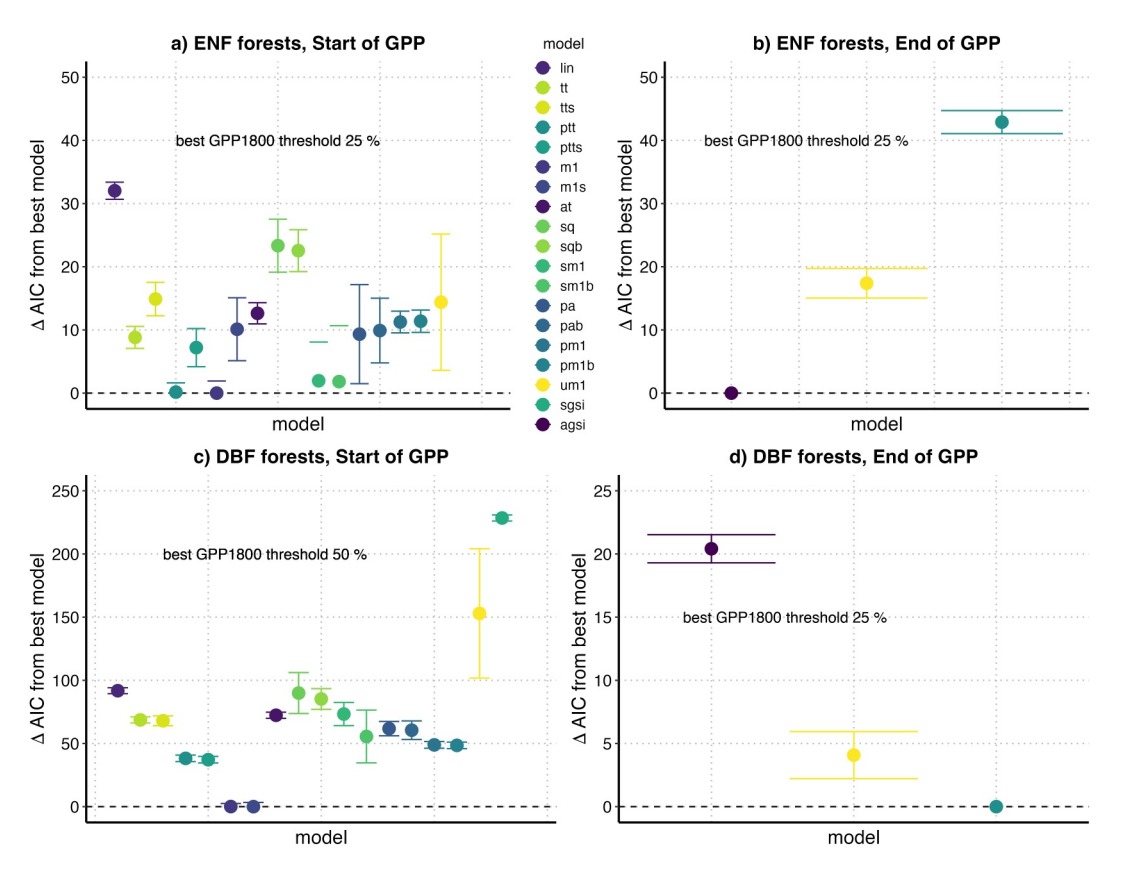


Figure 6. Comparison of difference in Akaike Information Criterion (Δ AIC) compared to the best-fit (lowest Akaike's Information Criterion) model in each case. Only the best GPP₁₈₀₀ thresholds from Figure S16 in Supporting Information S1 are shown. The SGSI and AGSI model results plot off scale (very high Δ AIC for Start_{GPP} for both evergreen needleleaf forests and deciduous broadleaf forests forests).

4. Discussion

4.1. Seasonal Timing of Photosynthesis and Dormancy

We used the light response of NEE to determine the timing of transitions from winter dormancy to photosynthetic activity and back. By exploiting the consistent soil T under a snowpack, we quantified the timing of end of snowmelt in spring, and start of snowpack accumulation in autumn. Our comparison revealed a robust and statistically significant difference in the phenology of GPP between evergreen and deciduous forests (Figure 4). Evergreen forests began photosynthesis in the spring well before end of snowmelt, approximately 3 weeks prior, while deciduous forests began photosynthesis about 4 weeks after end of snowmelt. Our hypothesis (H1) that snowmelt is required for initiation of photosynthesis received support for DBF, but ENF forests began photosynthesis well before snow was completely melted (Figures 3 and 4), thus refuting H1.

Validation of our snowpack timing method to derive Start_{snow} and End_{snow} is essential to ensure its reliability. Our validation efforts (Figures S5–S11 in Supporting Information S1) demonstrate the reliability of the method in defining the timing of the end of spring snowmelt to within 1–2 weeks. We acknowledge that snowmelt exhibits considerable spatial variability within a forest (e.g., Lundquist et al., 2013), and a single soil T measurement per site cannot represent the entire forest. Nevertheless, this uncertainty is much smaller than the observed difference in timing for Start_{GPP} between ENF and DBF forests, which is nearly 7 weeks (Figure 4e). As a priority for future research, we recommend that flux tower scientists in snowy locations incorporate automated measurements of SWE and snow depth, using snow pillows and ultrasonic depth sensors. A complementary alternative for automated depth measurement could be repeat digital photography (e.g., Richardson, 2019) with graduated snow stakes in the image. Continued development of remote sensing techniques to monitor snow over wide regions would also be valuable (e.g., Mavrovic et al., 2023; Metsämäki et al., 2015). SWE is the preferred metric because it provides information about the water available from the snowpack to support forest productivity (Hu

BOWLING ET AL. 15 of 25

com/doi/10.1029/2023JG007839 by University Of Utah Spencer S, Wiley Online Library on [27/04/2024]. See the Terms and Conditions (https://

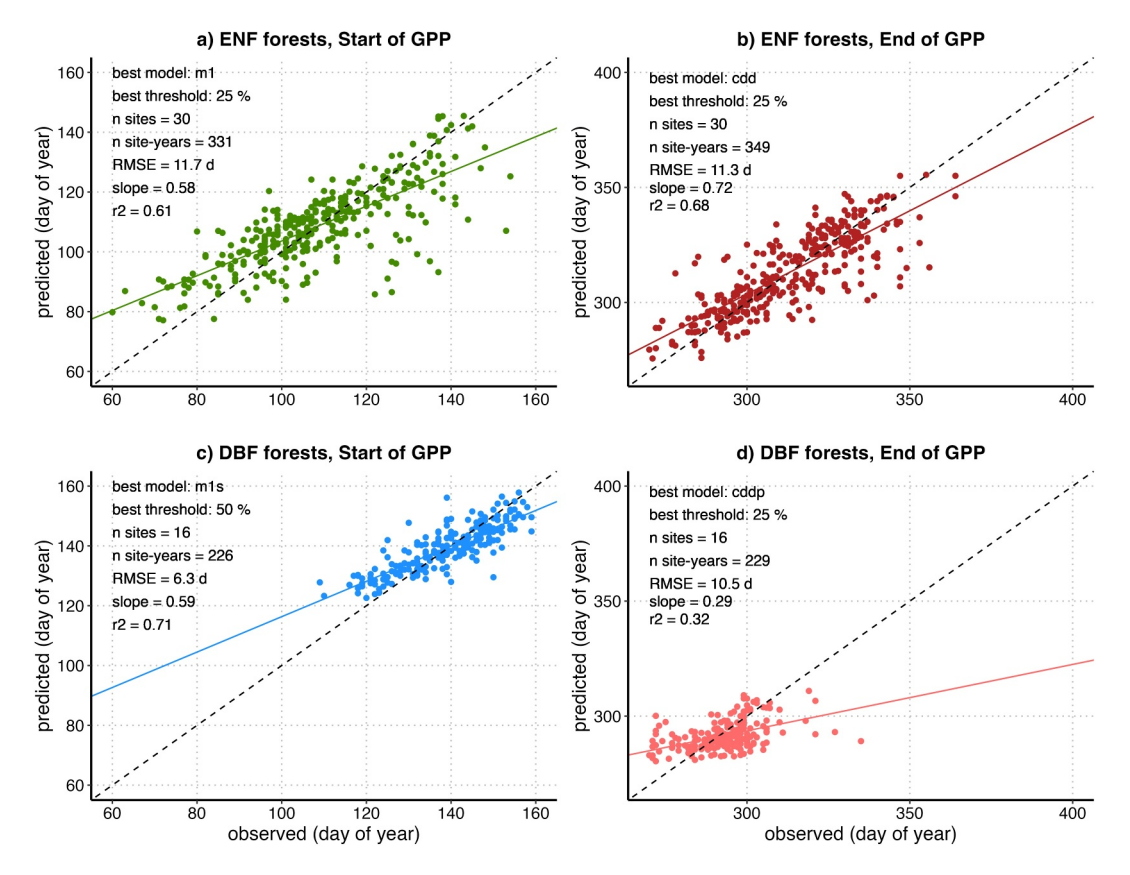


Figure 7. Comparison of predictions (vertical axes) of $Start_{GPP}$ and End_{GPP} from the best-fit phenology models (and associated GPP_{1800} thresholds, see Figure 6 and Figure S16 in Supporting Information S1) with the observed $Start_{GPP}$ and End_{GPP} (horizontal axes) derived from net ecosystem exchange and photosynthetically active radiation data as in Figure 1. Shown in each panel are the best model and GPP_{1800} threshold, number of sites and site-years represented, the root mean square error (predicted vs. observed), slope of a linear regression (colored lines), r^2 , and a 1:1 line for comparison.

et al., 2010; Maurer & Bowling, 2014). Measurements of T of the snowpack at multiple vertical and horizontal locations can be particularly useful to identify when and how rapidly the snow is melting (Burns et al., 2014; Jennings et al., 2018).

Our results provide new evidence supporting the general phenomenon of ENF photosynthesis commencing before the end of the snowmelt period, while DBF initiate photosynthesis afterward (Figures 3 and 4). This distinctive contrast between forest types aligns with earlier studies (Ahmed et al., 2021; Barr et al., 2009; Descals et al., 2020; Thum et al., 2009) The period between snowmelt and full development of canopy foliage in DBF forests has been referred to as the "vernal window" (Contosta et al., 2017; Groffman et al., 2012; Khodaee et al., 2022), and as climate warms, the length of the vernal window has increased (Contosta et al., 2017). In boreal regions, deciduous trees take up a surprisingly large amount of water during this phase, before leaf-out and full transpiration begins (Young-Robertson et al., 2016).

While evergreen forests must transport water through xylem once transpiration starts, accumulating evidence suggests that the initiation of transpiration in ENF forests lags behind photosynthesis, indicating the utilization of stored water for days to weeks (Bowling et al., 2018; Nehemy et al., 2022, 2023; Sevanto et al., 2006; Tanja et al., 2003). Notably, the rehydration of conifer stems following winter shrinkage can last several weeks (Nehemy et al., 2023; Turcotte et al., 2009). Our soil T method quantifies the end of the snowmelt period (End_{snow}), but cannot provide information about the start or duration of melt. The initiation and completion of soil thaw in spring can be markedly affected by forest structure (Ahmed et al., 2021; Lundquist et al., 2013). Soils in warmer locations may not freeze every winter, even under the snowpack (Iwata et al., 2010; Maurer & Bowling, 2014), and so thaw is not always a requirement for liquid water availability.

BOWLING ET AL. 16 of 25

We observed a substantial difference in the length of the photosynthesis season between ENF and DBF forests, as calculated using Start_{GPP} and End_{GPP} at the 10% threshold (Figure 4j). On average, the photosynthetically active season was approximately 50 days longer in ENF forests compared to DBF (Figure 4j). This confirms patterns identified for selected forests (Barr et al., 2009; Noormets et al., 2009) and early ecophysiological studies (Schulze et al., 1977). This disparity aligns with the relative length of carbon uptake period reported for these forest types by Churkina et al. (2005) and Panwar et al. (2023).

After photosynthesis began, the time taken for GPP to rise from 10% to 90% of maximum photosynthetic capacity in spring was nearly twice as fast for DBF compared to ENF forests (comparing means of the distributions in Figures 4a and 4e). The spring increase in photosynthetic capacity was termed the "recovery phase" by Gu et al. (2009), who showed faster recovery rate for 3 DBF forests compared to a single ENF forest. Yang and Noormets (2021) termed the period "length of flux development" and defined it using a GPP-based method to derive flux transition dates, but did not provide a quantitative description in their paper. Calculated from their data set, the spring ramp for ENF forests took 44 days (median of 40 forests, 300 site-years), while for DBF forests it lasted 28 days (22 forests, 185 site-years). This higher rate of spring increase in photosynthetic capacity by DBF forests also aligns with the seasonal patterns observed for ENF and DBF forests analyzed collectively by Panwar et al. (2023). Consequently, another generalizable phenological pattern emerges: ENF forests begin (end) photosynthesis earlier (later) but take nearly twice as long to reach peak photosynthetic capacity compared to DBF forests (Figure 4).

4.2. Lack of Long-Term Trends in Length of Photosynthesis Season

We hypothesized (H2) that climate warming has resulted in earlier start and later end of photosynthesis, consequently leading to a longer photosynthesis season. As described in the introduction, there is debate among flux-tower-based studies regarding changes in the timing of photosynthesis for deciduous and evergreen forests. We found no evidence in the flux tower data to support H2, a widespread directional pattern of change in Start_{GPP} or End_{GPP} for either evergreen or deciduous forests (Table S1, Figure S1 in Supporting Information S1). Out of the tested regressions of Start_{GPP} and End_{GPP} versus time, only a fraction (11%) yielded statistically significant trends (Table 2). Those that were significant did not show consistent patterns, as they exhibited earlier, later, and no change to the phenological transitions in both spring and autumn (the three methods to test for significance were not always in agreement). Since leaf T is strongly related to air T (Bowling et al., 2018; Leuzinger & Körner, 2007; Still et al., 2019), the lack of major trends in Start_{GPP} and End_{GPP} over time can potentially be explained by lack of long-term T change (but see next section).

Our findings align with other tower-based flux studies investigating flux phenology. Keenan et al. (2014) observed strong trends in start of season dates for the northeastern U.S. based on remote sensing of greenness (earlier spring by 0.5 days yr⁻¹), and showed that timing of spring and autumn transitions of C fluxes was strongly linked to T (see their Figures 3 and 5 and Figure S9 in Supporting Information S1). However, when analyzing flux tower data, they reported only marginally significant advances in spring GPP for Harvard Forest (US-Ha1) and for deciduous forests collectively. Moreover, no statistically significant trends were observed for GPP nor NEE timing in coniferous forests. Finzi et al. (2020) extended these results for Harvard Forest, reporting a trend of 0.4 days yr⁻¹ for the DBF tower (US-Ha1), but found no significant trends for the ENF tower (US-Ha2, see their Figure 12). Panwar et al. (2023) identified significant trends only for lower thresholds (akin to our GPP₁₈₀₀ thresholds) and only when ENF and DBF forests were analyzed as groups, rather than as individual forests. At Hyytiälä (FI-Hyy), Launiainen et al. (2022) found a weak but marginally significant trend for earlier start of the GPP season (see their Table 2). Finally, Wang et al. (2019) reported no change in spring or autumn timing of C fluxes during the global warming hiatus (1998–2012) using FLUXNET data. Our study, along with the aforementioned research, presents a direct contrast to the findings of Xu et al. (2019) who reported highly significant trends toward earlier spring and autumn transitions in both forest types (their Table 1).

The above studies either focused on time series of GPP derived from flux partitioning, or of NEE. Our approach to determine transition dates (Figure 1, Figure S3 in Supporting Information S1) instead relies on the functional relation between NEE and sunlight. This distinction allows us to avoid the problematic artifact of erroneous winter GPP that arises from flux partitioning (Figure S2 in Supporting Information S1). Our record extends the analysis of Wang et al. (2019) by 6+ years (Figure S1, Table S1 in Supporting Information S1) with added forest sites, uses an entirely different method, and we reach the same conclusion. Specifically, we find no compelling

BOWLING ET AL. 17 of 25

evidence to support a general change in the timing of spring or autumn C fluxes in the northern hemisphere forest flux tower record, with a few exceptions (Table 2), thus refuting H2 at the long-term time scale.

4.3. Evaluation of Phenological Model Performance

We assessed the predictive capacity of a variety of phenological models to determine Start_{GPP} and End_{GPP}. The goal was to test (H3) if simple models based on gridded weather data could predict the phenology of photosynthesis, and therefore should be incorporated in future TBMs. For DBF, the most effective spring models were the M1s and M1 models (Figure 6c). These models predicted Start_{GPP} favorably across all 16 DBF forests with an RMSE of 6.3 days (226 site-years, Figure 7c). This level of predictive model skill is comparable to lowest prediction errors when these models were applied to predict leaf unfolding (Basler, 2016; Migliavacca et al., 2012). However, for modeling spring green-up of evergreen forests across the Northeastern US, Teets et al. (2023) found that the M1 model was out-performed by parallel and sequential models that incorporated chilling effects. A plausible interpretation of these differing outcomes is that, given the large geographic range covered by our study sites, parallel and sequential models might not perform as effectively without regional calibration of chilling thresholds. In contrast, the photoperiod-temperature structure inherent in the M1s and M1 models retained its generalizability across different spatial and temporal contexts.

For ENF, the most effective spring models included M1 but also PTT, SM1, and SM1b, with nearly equal performance based on AIC (Figure 6a). Both M1 and PTT include accumulated T and photoperiod (Črepinšek et al., 2006) with minor difference in form. The SM1 and SM1b models also include a chilling threshold which must be satisfied before early spring T accumulation can initiate leaf unfolding, hence the "sequential" name (Hänninen, 1990; Kramer, 1994). Although the AIC difference was minimal, model complexity differs. The SM1 and SM1b models have 9 parameters, compared to 4 (M1) and 3 (PTT), and the principle of parsimony suggests that M1 and PTT may be preferable due to their simplicity. Model prediction across 30 ENF forests had RMSE of 11.7 days (331 site years, Figure 7a). This is similar in magnitude to the interannual variability in Start_{GPP} for most forests (Figure 3). In summary, for ENF forests in spring, these results suggest that we can reduce the number of useful candidate models in future studies from 15 (as listed in Table 1) to 4 promising models (M1, PTT, SM1, SM1b).

The timing of the autumn transition for ENF forests was best modeled with the CDD model, which was developed to predict autumn leaf color transitions in deciduous forests (Jeong & Medvigy, 2014). This model is a simple accumulation of cold (air T) below a site-specific base T, until a chilling threshold is met. Model selection, guided by AIC, favored the CDD model in ENF forests; this is consistent with Schädel et al. (2023) who found that the CDD model was most effective for the autumn transition in *Picea mariana* at the NGEE-SPRUCE experiment (warming of up to +9°C above ambient). This model yielded RMSE of 11.3 days for autumn prediction (Figure 7b).

For DBF forests, adding a photoperiod threshold to the chilling algorithm led to the best prediction in autumn via the CDDP model (Jeong & Medvigy, 2014), with RMSE of 10.5 days (Figure 7d). In contrast to ENF, there was more support for the CDDP model in DBF forests. This contrasts with the results of Teets et al. (2023) for modeling the start of autumn senescence in deciduous forests of the Northeastern U.S., but this is likely related to the distinction between "start of senescence" and "end of photosynthesis."

Importantly, our results indicate that existing phenology models can predict the timing of the start of photosynthesis in spring, or its end in autumn, with an average accuracy of approximately 10 days. Notably, these models were not driven by weather data directly collected at the flux towers but rather by widely adopted gridded weather data products (Cornes et al., 2018; Thornton et al., 2021), and thus can be easily incorporated into TBMs.

We did not find evidence for long-term change in Start_{GPP} or End_{GPP} in the flux record (Section 4.2), but the model results indicate that accumulated T is the primary control on interannual variability of phenology in both spring and autumn, with photoperiod as a secondary control in spring. Keenan et al. (2014) showed that the timing of the start of photosynthesis in spring was dependent on the spring T anomaly (their Figure 5 and Figure S10 in Supporting Information S1), with warmer spring T leading to earlier start. Further synthesis of evergreen flux tower sites showed that warmer springs advanced onset of photosynthetic uptake, and warmer autumns delayed its end (Richardson et al., 2018). Our results are in complete agreement. Interannual variation in Start_{GPP} or End_{GPP} was strongly linked to interannual variation in air T (Figure 5). Collectively, the observational and modeling results of the present study provide strong support for the hypothesis that future climate warming is likely to lead to earlier start of photosynthesis and a potentially longer photosynthesis season.

BOWLING ET AL. 18 of 25

Acknowledgments

Thanks to the worldwide flux tower

community for collecting, processing,

innovating, and curating data access for all. Special thanks to a few valued colleagues

who were not able to collaborate due to government restrictions. We are also

grateful to the USDA NRCS Snow Survey Program for sharing data. This research

was funded by the U.S. National Science Foundation Macrosystems Biology and

NEON-Enabled Science (awards 1926090

and 1702697), Division of Environmental Biology programs (award 1929709), and

Long-Term Ecological Research Program

(1832210) grants. Some computational analyses were run on Northern Arizona University's Monsoon computing cluster, funded by Arizona's Technology and

Research Initiative Fund. Additional funding for ongoing data collection was

provided by: the U.S. Dept. of Energy

core site, the U.S. Dept. of Agriculture Forest Service, the Arctic Challenge for

Sustainability II (JPMXD1420318865,

(GA 871128), the Italian Integrated

Environmental Research Infrastructures Systems (ITINERIS, IR0000032), Forest

Services of Autonomous Province of

Bolzano, ICOS Denmark, LTER Denmark,

ICOS-Finland, Academy of Finland, EU Horizon-Europe project GreenFeedback

(Grant 10105692), Ministry of Education,

Youth, and Sports of the Czech Republic

within the National Infrastructure for

Carbon Observations-CzeCOS (No.

Foundation (project 21-14-00209).

LM2023048), and the Russian Science

Japan), the European Commission eLTER H2020 (GA 654359) and eLTER PLUS

AmeriFlux Network Management Project support to ChEAS, UMBS, and US-NR1

4.4. Implications for Terrestrial Biosphere Modeling

Most ecosystem, land-surface, and TBMs have been developed with emphasis on representing underlying processes. In the Community Land Model, for example, for DBF there are phenological subroutines driven by air and soil T, and daylength that control budburst, leaf emergence, and canopy development in spring (the "onset" period in CLM), and senescence and leaf drop in autumn (the "offset period," https://www2.cesm.ucar.edu/models/cesm2/land/CLM50_Tech_Note.pdf, Lawrence et al., 2019). Photosynthesis is then modeled as a function of leaf area, modulated by incoming solar radiation, T, and humidity. The phenology of photosynthesis, defined by the start and end dates of photosynthetic activity, emerges indirectly through this representation. By comparison, for ENF, where leaf area is present year-round, photosynthesis can in principle occur any time conditions are favorable. CLM allows seasonal variation in photosynthetic electron transport rate (J_{max}) and carboxylation velocity (V_{cmax}) as a function of daylength and air T. Thus, there is a built-in model capability for photosynthetic capacity to have its own seasonal rhythm, but the parameterization is arguably coarse, at best.

The seasonality of evergreen needleleaf photosynthesis, as well as up- and down-regulation of photosynthetic capacity and photoprotection, is driven by T and photoperiod (Ensminger et al., 2004; Fréchette et al., 2016; Tanja et al., 2003), consistent with the M1 and CDD models used here. Given the ability of these models to describe broad spatial patterns in photosynthetic phenology of ENF, there is clearly potential to include a more explicit, process-oriented, if not explicitly process-based, representation of evergreen photosynthetic phenology in TBMs. For example, the M1 and CDD models could be used as switches in spring and autumn, turning off and on the dormancy of the photosynthetic machinery. While all models are imperfect, such changes would almost certainly improve on the large errors in modeling evergreen photosynthetic phenology by TBMs that have been reported previously (Richardson et al., 2012). Additionally, because of the inherent coupling between photosynthesis and transpiration, improving the seasonality of photosynthesis in simulation models would also contribute to better representation of evapotranspiration and thus the surface energy balance, both critically important as regulators of land-atmosphere interactions related to the boundary layer, precipitation, and atmospheric transport (Peano et al., 2021; Richardson et al., 2013).

Data Availability Statement

Flux tower data used in this study are freely available from the AmeriFlux (https://ameriflux.lbl.gov/), FLUX-NET2015 (https://fluxnet.org/data/fluxnet2015-dataset/), and Warm Winter 2020 (https://www.icos-cp.eu/data-products/2G60-ZHAK) databases. Gridded weather data are available from Daymet (https://daymet.ornl.gov/and E-OBS (https://www.ecad.eu/download/ensembles/ensembles.php). Dates for Start_{GPP}, End_{GPP}, Start_{snow}, and End_{snow} from our study, and R scripts to calculate these dates, are included in the supplemental material.

References

Ahmed, H. F., Helgason, W., Barr, A., & Black, A. (2021). Characterization of spring thaw and its relationship with carbon uptake for different types of southern boreal forest. Agricultural and Forest Meteorology, 307, 108511. https://doi.org/10.1016/j.agrformet.2021. 108511

Amiro, B. (2010). Estimating annual carbon dioxide eddy fluxes using open-path analysers for cold forest sites. Agricultural and Forest Meteorology, 150(10), 1366–1372. https://doi.org/10.1016/j.agrformet.2010.06.007

Bailey, K., Szejner, P., Strange, B., Monson, R. K., & Hu, J. (2023). The influence of winter snowpack on the use of summer rains in montane pine forests across the southwest US. *Journal of Geophysical Research: Biogeosciences*, 128(9), e2023JG007494. https://doi.org/10.1029/2023JG007494

Barichivich, J., Briffa, K. R., Myneni, R. B., Osborn, T. J., Melvin, T. M., Ciais, P., et al. (2013). Large-scale variations in the vegetation growing season and annual cycle of atmospheric CO₂ at high northern latitudes from 1950 to 2011. *Global Change Biology*, 19(10), 3167–3183. https://doi.org/10.1111/gcb.12283

Barr, A., Black, T. A., & McCaughey, H. (2009). Climatic and phenological controls of the carbon and energy balances of three contrasting boreal forest ecosystems in western Canada. In A. Noormets (Ed.), *Phenology of ecosystem processes* (pp. 3–34). Springer. https://doi.org/10.1007/978-1-4419-0026-5 1

Basler, D. (2016). Evaluating phenological models for the prediction of leaf-out dates in six temperate tree species across central Europe. Agricultural and Forest Meteorology, 217, 10–21. https://doi.org/10.1016/j.agrformet.2015.11.007

Beniston, M., Farinotti, D., Stoffel, M., Andreassen, L. M., Coppola, E., Eckert, N., et al. (2018). The European mountain cryosphere: A review of its current state, trends, and future challenges. *The Cryosphere*, 12(2), 759–794. https://doi.org/10.5194/tc-12-759-2018

Black, T. A., Chen, W. J., Barr, A. G., Arain, M. A., Chen, Z., Nesic, Z., et al. (2000). Increased carbon sequestration by a boreal deciduous forest in years with a warm spring. *Geophysical Research Letters*, 27(9), 1271–1274. https://doi.org/10.1029/1999GL011234

Blümel, K., & Chmielewski, F.-M. (2012). Shortcomings of classical phenological forcing models and a way to overcome them. *Agricultural and Forest Meteorology*, 164, 10–19. https://doi.org/10.1016/j.agrformet.2012.05.001

BOWLING ET AL. 19 of 25

- Bowling, D. R., Logan, B. A., Hufkens, K., Aubrecht, D. M., Richardson, A. D., Burns, S. P., et al. (2018). Limitations to winter and spring photosynthesis of a Rocky Mountain subalpine forest. *Agricultural and Forest Meteorology*, 252, 241–255. https://doi.org/10.1016/j.agrformet.2018.01.025
- Brandt, J. P. (2009). The extent of the North American boreal zone. *Environmental Reviews*, 17(NA), 101–161. https://doi.org/10.1139/A09-004 Buermann, W., Bikash, P. R., Jung, M., Burn, D. H., & Reichstein, M. (2013). Earlier springs decrease peak summer productivity in North American boreal forests. *Environmental Research Letters*, 8(2), 024027. https://doi.org/10.1088/1748-9326/8/2/024027
- Burba, G. G., McDERMITT, D. K., Grelle, A., Anderson, D. J., & Xu, L. (2008). Addressing the influence of instrument surface heat exchange on the measurements of CO₂ flux from open-path gas analyzers. *Global Change Biology*, 14(8), 1854–1876. https://doi.org/10.1111/j.1365-2486. 2008.01606.x
- Burnham, K. P., & Anderson, D. R. (2004). Multimodel inference: Understanding AIC and BIC in model selection. Sociological Methods & Research, 33(2), 261–304. https://doi.org/10.1177/0049124104268644
- Burns, S. P., Molotch, N. P., Williams, M. W., Knowles, J. F., Seok, B., Monson, R. K., et al. (2014). Snow temperature changes within a seasonal snowpack and their relationship to turbulent fluxes of sensible and latent heat. *Journal of Hydrometeorology*, 15(1), 117–142. https://doi.org/10.1175/JHM-D-13-026.1
- Calinger, K., & Curtis, P. (2023). A century of climate warming results in growing season extension: Delayed autumn leaf phenology in north central North America. PLoS One, 18(3), e0282635. https://doi.org/10.1371/journal.pone.0282635
- Cannell, M. G. R., & Smith, R. I. (1983). Thermal time, chill days and prediction of budburst in Picea sitchensis. *Journal of Applied Ecology*, 20(3), 951–963. https://doi.org/10.2307/2403139
- Chen, B. (2022). Comparison of the two most common phenology algorithms imbedded in land surface models. *Journal of Geophysical Research:* Atmospheres, 127(21), e2022JD037167. https://doi.org/10.1029/2022JD037167
- Chen, M., Melaas, E. K., Gray, J. M., Friedl, M. A., & Richardson, A. D. (2016). A new seasonal-deciduous spring phenology submodel in the Community Land Model 4.5: Impacts on carbon and water cycling under future climate scenarios. *Global Change Biology*, 22(11), 3675–3688. https://doi.org/10.1111/gcb.13326
- Chuine, I., Cour, P., & Rousseau, D. D. (1998). Fitting models predicting dates of flowering of temperate-zone trees using simulated annealing. Plant, Cell and Environment, 21(5), 455–466. https://doi.org/10.1046/j.1365-3040.1998.00299.x
- Chuine, I., Cour, P., & Rousseau, D. D. (1999). Selecting models to predict the timing of flowering of temperate trees: Implications for tree phenology modelling. *Plant, Cell and Environment*, 22(1), 1–13. https://doi.org/10.1046/j.1365-3040.1999.00395.x
- Chuine, I., & Régnière, J. (2017). Process-based models of phenology for plants and animals. Annual Review of Ecology Evolution and Systematics, 48(1), 159–182. https://doi.org/10.1146/annurev-ecolsys-110316-022706
- Chuine, I. (2000). A unified model for budburst of trees. *Journal of Theoretical Biology*, 207(3), 337–347. https://doi.org/10.1006/jtbi.2000.2178 Churkina, G., Schimel, D., Braswell, B. H., & Xiao, X. (2005). Spatial analysis of growing season length control over net ecosystem exchange. *Global Change Biology*, 11(10), 1777–1787. https://doi.org/10.1111/j.1365-2486.2005.001012.x
- Clare, R. M., Desai, A. R., Martin, J. E., Notaro, M., & Vavrus, S. J. (2023). Extratropical cyclone response to projected reductions in snow extent over the great plains. *Atmosphere*, 14(5), 783. https://doi.org/10.3390/atmos14050783
- Contosta, A. R., Adolph, A., Burchsted, D., Burakowski, E., Green, M., Guerra, D., et al. (2017). A longer vernal window: The role of winter coldness and snowpack in driving spring transitions and lags. Global Change Biology, 23(4), 1610–1625. https://doi.org/10.1111/gcb.13517
- Cornes, R. C., van der Schrier, G., van den Besselaar, E. J. M., & Jones, P. D. (2018). An ensemble version of the E-OBS temperature and precipitation data sets. *Journal of Geophysical Research: Atmospheres*, 123(17), 9391–9409. https://doi.org/10.1029/2017JD028200
- Črepinšek, Z., Kajfež-Bogataj, L., & Bergant, K. (2006). Modelling of weather variability effect on fitophenology. *Ecological Modelling*, 194(1), 256–265. https://doi.org/10.1016/j.ecolmodel.2005.10.020
- Desai, A. R., Murphy, B. A., Wiesner, S., Thom, J., Butterworth, B. J., Koupaei-Abyazani, N., et al. (2022). Drivers of decadal carbon fluxes across temperate ecosystems. *Journal of Geophysical Research: Biogeosciences*, 127(12), e2022JG007014. https://doi.org/10.1029/2022JG007014
- Descals, A., Verger, A., Filella, I., Baldocchi, D., Janssens, I. A., Fu, Y. H., et al. (2020). Soil thawing regulates the spring growth onset in tundra and alpine biomes. Science of the Total Environment, 742, 140637. https://doi.org/10.1016/j.scitotenv.2020.140637
- Ensminger, I., Sveshnikov, D., Campbell, D. A., Funk, C., Jansson, S., Lloyd, J., et al. (2004). Intermittent low temperatures constrain spring recovery of photosynthesis in boreal Scots pine forests. *Global Change Biology*, *10*(6), 995–1008. https://doi.org/10.1111/j.1365-2486.2004.
- Finzi, A. C., Giasson, M.-A., Barker Plotkin, A. A., Aber, J. D., Boose, E. R., Davidson, E. A., et al. (2020). Carbon budget of the Harvard forest long-term ecological research site: Pattern, process, and response to global change. *Ecological Monographs*, 90(4), e01423. https://doi.org/10.1002/ecm.1423
- Fréchette, E., Chang, C. Y.-Y., & Ensminger, I. (2016). Photoperiod and temperature constraints on the relationship between the photochemical reflectance index and the light use efficiency of photosynthesis in Pinus strobus. *Tree Physiology*, 36(3), 311–324. https://doi.org/10.1093/treephys/tpv143
- Friedlingstein, P., Jones, M. W., O'Sullivan, M., Andrew, R. M., Bakker, D. C. E., Hauck, J., et al. (2022). Global carbon budget 2021. Earth System Science Data, 14(4), 1917–2005. https://doi.org/10.5194/essd-14-1917-2022
- Friedlingstein, P., Meinshausen, M., Arora, V. K., Jones, C. D., Anav, A., Liddicoat, S. K., & Knutti, R. (2014). Uncertainties in CMIP5 climate projections due to carbon cycle feedbacks. *Journal of Climate*, 27(2), 511–526. https://doi.org/10.1175/JCLI-D-12-00579.1
- Garrity, S. R., Bohrer, G., Maurer, K. D., Mueller, K. L., Vogel, C. S., & Curtis, P. S. (2011). A comparison of multiple phenology data sources for estimating seasonal transitions in deciduous forest carbon exchange. *Agricultural and Forest Meteorology*, 151(12), 1741–1752. https://doi.org/10.1016/j.agrformet.2011.07.008
- Gauthier, S., Bernier, P., Kuuluvainen, T., Shvidenko, A. Z., & Schepaschenko, D. G. (2015). Boreal forest health and global change. *Science*, 349(6250), 819–822. https://doi.org/10.1126/science.aaa9092
- Goldsmith, G. R., Allen, S. T., Braun, S., Siegwolf, R. T. W., & Kirchner, J. W. (2022). Climatic influences on summer use of winter precipitation by trees. *Geophysical Research Letters*, 49(10), e2022GL098323. https://doi.org/10.1029/2022GL098323
- Graf, A., Wohlfahrt, G., Aranda-Barranco, S., Arriga, N., Brümmer, C., Ceschia, E., et al. (2023). Joint optimization of land carbon uptake and albedo can help achieve moderate instantaneous and long-term cooling effects. *Communications Earth & Environment*, 4(1), 1–12. https://doi.org/10.1038/s43247-023-00958-4
- Groffman, P. M., Driscoll, C. T., Fahey, T. J., Hardy, J. P., Fitzhugh, R. D., & Tierney, G. L. (2001). Colder soils in a warmer world: A snow manipulation study in a northern hardwood forest ecosystem. *Biogeochemistry*, 56(2), 135–150. https://doi.org/10.1023/a:1013039830323

BOWLING ET AL. 20 of 25

- Groffman, P. M., Rustad, L. E., Templer, P. H., Campbell, J. L., Christenson, L. M., Lany, N. K., et al. (2012). Long-term integrated studies show complex and surprising effects of climate change in the northern hardwood forest. *BioScience*, 62(12), 1056–1066. https://doi.org/10.1525/bio.2012.62.12.7
- Gu, H., Qiao, Y., Xi, Z., Rossi, S., Smith, N. G., Liu, J., & Chen, L. (2022). Warming-induced increase in carbon uptake is linked to earlier spring phenology in temperate and boreal forests. *Nature Communications*, 13(1), 3698. https://doi.org/10.1038/s41467-022-31496-w
- Gu, L., Post, W. M., Baldocchi, D. D., Black, T. A., Suyker, A. E., Verma, S. B., et al. (2009). Characterizing the seasonal dynamics of plant community photosynthesis across a range of vegetation types. In A. Noormets (Ed.), *Phenology of ecosystem processes* (pp. 35–58). Springer. https://doi.org/10.1007/978-1-4419-0026-5_2
- Hänninen, H. (1990). Modelling bud dormancy release in trees from cool and temperate regions. Silva Fennica, 0(213). https://doi.org/10.14214/aff.7660
- Hänninen, H., Kramer, K., Tanino, K., Zhang, R., Wu, J., & Fu, Y. H. (2018). Experiments are necessary in process-based tree phenology modelling. *Trends in Plant Science*, 24(3), 199–209. https://doi.org/10.1016/j.tplants.2018.11.006
- Hollinger, D. Y., Davidson, E. A., Fraver, S., Hughes, H., Lee, J. T., Richardson, A. D., et al. (2021). Multi-Decadal carbon cycle measurements indicate resistance to external drivers of change at the Howland forest AmeriFlux site. *Journal of Geophysical Research: Biogeosciences*, 126(8), e2021JG006276. https://doi.org/10.1029/2021JG006276
- Hollinger, D. Y., Goltz, S. M., Davidson, E. A., Lee, J. T., Tu, K., & Valentine, H. T. (1999). Seasonal patterns and environmental control of carbon dioxide and water vapour exchange in an ecotonal boreal forest. *Global Change Biology*, 5(8), 891–902. https://doi.org/10.1046/j.1365-2486.1999.00281.x
- Hu, J., Moore, D. J. P., Burns, S. P., & Monson, R. K. (2010). Longer growing seasons lead to less carbon sequestration by a subalpine forest. Global Change Biology, 16(2), 771–783. https://doi.org/10.1111/j.1365-2486.2009.01967.x
- Hufkens, K., Basler, D., Milliman, T., Melaas, E. K., & Richardson, A. D. (2018). An integrated phenology modelling framework in r. Methods in Ecology and Evolution, 9(5), 1276–1285. https://doi.org/10.1111/2041-210X.12970
- Hunter, A. F., & Lechowicz, M. J. (1992). Predicting the timing of budburst in temperate trees. *Journal of Applied Ecology*, 29(3), 597–604. https://doi.org/10.2307/2404467
- Hurdebise, Q., Aubinet, M., Heinesch, B., & Vincke, C. (2019). Increasing temperatures over an 18-year period shortens growing season length in a beech (Fagus sylvatica L.)-dominated forest. *Annals of Forest Science*, 76(3), 75. https://doi.org/10.1007/s13595-019-0861-8
- Iwata, Y., Hirota, T., Hayashi, M., Suzuki, S., & Hasegawa, S. (2010). Effects of frozen soil and snow cover on cold-season soil water dynamics in Tokachi, Japan. *Hydrological Processes*, 24(13), 1755–1765. https://doi.org/10.1002/hyp.7621
- Jennings, K. S., Kittel, T. G. F., & Molotch, N. P. (2018). Observations and simulations of the seasonal evolution of snowpack cold content and its relation to snowmelt and the snowpack energy budget. *The Cryosphere*, 12(5), 1595–1614. https://doi.org/10.5194/tc-12-1595-2018
- Jeong, S.-J., Ho, C.-H., Gim, H.-J., & Brown, M. E. (2011). Phenology shifts at start vs. end of growing season in temperate vegetation over the Northern Hemisphere for the period 1982–2008. *Global Change Biology*, 17(7), 2385–2399. https://doi.org/10.1111/j.1365-2486.2011.
- Jeong, S.-J., & Medvigy, D. (2014). Macroscale prediction of autumn leaf coloration throughout the continental United States. Global Ecology and Biogeography, 23(11), 1245–1254. https://doi.org/10.1111/geb.12206
- Keenan, R. J., Reams, G. A., Achard, F., de Freitas, J. V., Grainger, A., & Lindquist, E. (2015). Dynamics of global forest area: Results from the FAO Global Forest Resources Assessment 2015. Forest Ecology and Management, 352, 9–20. https://doi.org/10.1016/j.foreco.2015.06.014
- Keenan, T. F., Gray, J., Friedl, M. A., Toomey, M., Bohrer, G., Hollinger, D. Y., et al. (2014). Net carbon uptake has increased through warming-induced changes in temperate forest phenology. *Nature Climate Change*, 4(7), 598–604. https://doi.org/10.1038/nclimate2253
- Khodaee, M., Hwang, T., Ficklin, D. L., & Duncan, J. M. (2022). With warming, spring streamflow peaks are more coupled with vegetation greenup than snowmelt in the northeastern United States. *Hydrological Processes*, 36(6), e14621. https://doi.org/10.1002/hyp.14621
- Klein, G., Vitasse, Y., Rixen, C., Marty, C., & Rebetez, M. (2016). Shorter snow cover duration since 1970 in the Swiss Alps due to earlier snowmelt more than to later snow onset. Climatic Change, 139(3), 637–649. https://doi.org/10.1007/s10584-016-1806-y
- Knowles, J. F., Molotch, N. P., Trujillo, E., & Litvak, M. E. (2018). Snowmelt-driven trade-offs between early and late season productivity negatively impact forest carbon uptake during drought. *Geophysical Research Letters*, 45(7), 3087–3096. https://doi.org/10.1002/ 2017GL076504
- Kobayashi, H., Yunus, A. P., Nagai, S., Sugiura, K., Kim, Y., Van Dam, B., et al. (2016). Latitudinal gradient of spruce forest understory and tundra phenology in Alaska as observed from satellite and ground-based data. *Remote Sensing of Environment*, 177, 160–170. https://doi.org/10.1016/j.rse.2016.02.020
- Kong, D., Zhang, Y., Wang, D., Chen, J., & Gu, X. (2020). Photoperiod explains the asynchronization between vegetation carbon phenology and vegetation greenness phenology. *Journal of Geophysical Research: Biogeosciences*, 125(8), e2020JG005636. https://doi.org/10.1029/2020JG005636
- Kramer, K. (1994). Selecting a model to predict the onset of growth of Fagus sylvatica. *Journal of Applied Ecology*, 31(1), 172–181. https://doi.org/10.2307/2404609
- Kunik, L., Bowling, D. R., Raczka, B., Frankenberg, C., Köhler, P., Cheng, R., et al. (2023). Satellite-based solar-induced fluorescence tracks seasonal and elevational patterns of photosynthesis in California's Sierra Nevada mountains. *Environmental Research Letters*, 19(1), 014008. https://doi.org/10.1088/1748-9326/ad07b4
- Kurz, W. A., Shaw, C. H., Boisvenue, C., Stinson, G., Metsaranta, J., Leckie, D., et al. (2013). Carbon in Canada's boreal forest—A synthesis. Environmental Reviews, 21(4), 260–292. https://doi.org/10.1139/er-2013-0041
- Landsberg, J. J. (1974). Apple fruit bud development and growth; analysis and an empirical model. *Annals of Botany*, 38(158), 1013–1023. https://doi.org/10.1093/oxfordjournals.aob.a084891
- Launiainen, S., Katul, G. G., Leppä, K., Kolari, P., Aslan, T., Grönholm, T., et al. (2022). Does growing atmospheric CO₂ explain increasing carbon sink in a boreal coniferous forest? *Global Change Biology*, 28(9), 2910–2929. https://doi.org/10.1111/gcb.16117
- Lawrence, D. M., Fisher, R. A., Koven, C. D., Oleson, K. W., Swenson, S. C., Bonan, G., et al. (2019). The community land model version 5: Description of new features, benchmarking, and impact of forcing uncertainty. *Journal of Advances in Modeling Earth Systems*, 11(12), 4245–4287. https://doi.org/10.1029/2018MS001583
- Leuzinger, S., & Körner, C. (2007). Tree species diversity affects canopy leaf temperatures in a mature temperate forest. Agricultural and Forest Meteorology, 146(1–2), 29–37. https://doi.org/10.1016/j.agrformet.2007.05.007
- Li, X., Ault, T., Richardson, A. D., Carrillo, C. M., Lawrence, D. M., Lombardozzi, D., et al. (2023). Impacts of shifting phenology on boundary layer dynamics in North America in the CESM. *Agricultural and Forest Meteorology*, 330, 109286. https://doi.org/10.1016/j.agrformet.2022. 109286

BOWLING ET AL. 21 of 25

- Li, X., Melaas, E., Carrillo, C. M., Ault, T., Richardson, A. D., Lawrence, P., et al. (2022). A comparison of land surface phenology in the northern hemisphere derived from satellite remote sensing and the community land model. *Journal of Hydrometeorology*, 23(6), 859–873. https://doi.org/10.1175/JHM-D-21-0169.1
- Linderholm, H. W. (2006). Growing season changes in the last century. Agricultural and Forest Meteorology, 137(1), 1–14. https://doi.org/10.1016/j.agrformet.2006.03.006
- Lundquist, J. D., Dickerson-Lange, S. E., Lutz, J. A., & Cristea, N. C. (2013). Lower forest density enhances snow retention in regions with warmer winters: A global framework developed from plot-scale observations and modeling. *Water Resources Research*, 49(10), 6356–6370. https://doi.org/10.1002/wrcr.20504
- Luyssaert, S., Inglima, I., Jung, M., Richardson, A. D., Reichstein, M., Papale, D., et al. (2007). CO₂ balance of boreal, temperate, and tropical forests derived from a global database. *Global Change Biology*, 13(12), 2509–2537. https://doi.org/10.1111/j.1365-2486.2007.01439.x
- Magney, T. S., Bowling, D. R., Logan, B. A., Grossmann, K., Stutz, J., Blanken, P. D., et al. (2019). Mechanistic evidence for tracking the seasonality of photosynthesis with solar-induced fluorescence. *Proceedings of the National Academy of Sciences*, 116(24), 11640–11645. https://doi.org/10.1073/pnas.1900278116
- Masle, J., Doussinault, G., Farquhar, G. D., & Sun, B. (1989). Foliar stage in wheat correlates better to photothermal time than to thermal time. *Plant, Cell and Environment*, 12(3), 235–247. https://doi.org/10.1111/j.1365-3040.1989.tb01938.x
- Maurer, G. E., & Bowling, D. R. (2014). Seasonal snowpack characteristics influence soil temperature and water content at multiple scales in interior western US mountain ecosystems. Water Resources Research, 50(6), 5216–5234. https://doi.org/10.1002/2013WR014452
- Mavrovic, A., Sonnentag, O., Lemmetyinen, J., Baltzer, J. L., Kinnard, C., & Roy, A. (2023). Reviews and syntheses: Recent advances in microwave remote sensing in support of terrestrial carbon cycle science in Arctic-boreal regions. *Biogeosciences*, 20(14), 2941–2970. https://doi.org/10.5194/bg-20-2941-2023
- McGuire, A. D., Chapin, F. S., Walsh, J. E., & Wirth, C. (2006). Integrated regional changes in Arctic climate feedbacks: Implications for the global climate system. *Annual Review of Environment and Resources*, 31(1), 61–91. https://doi.org/10.1146/annurev.energy.31.020105. 100253
- Melaas, E. K., Friedl, M. A., & Richardson, A. D. (2016). Multiscale modeling of spring phenology across deciduous forests in the Eastern United States. *Global Change Biology*, 22(2), 792–805. https://doi.org/10.1111/gcb.13122
- Menzel, A., Sparks, T. H., Estrella, N., Koch, E., Aasa, A., Ahas, R., et al. (2006). European phenological response to climate change matches the warming pattern. *Global Change Biology*, 12(10), 1969–1976. https://doi.org/10.1111/j.1365-2486.2006.01193.x
- Metsämäki, S., Pulliainen, J., Salminen, M., Luojus, K., Wiesmann, A., Solberg, R., et al. (2015). Introduction to GlobSnow Snow Extent products with considerations for accuracy assessment. Remote Sensing of Environment, 156, 96–108. https://doi.org/10.1016/j.rse.2014.09.018
- Migliavacca, M., Sonnentag, O., Keenan, T. F., Cescatti, A., O'Keefe, J., & Richardson, A. D. (2012). On the uncertainty of phenological responses to climate change, and implications for a terrestrial biosphere model. *Biogeosciences*, 9(6), 2063–2083. https://doi.org/10.5194/bg-9-2063-2012
- Mioduszewski, J. R., Rennermalm, A. K., Robinson, D. A., & Wang, L. (2015). Controls on spatial and temporal variability in northern hemisphere terrestrial snow melt timing, 1979–2012. *Journal of Climate*, 28(6), 2136–2153. https://doi.org/10.1175/JCLI-D-14-00558.1
- Monson, R. K., Sparks, J. P., Rosenstiel, T. N., Scott-Denton, L. E., Huxman, T. E., Harley, P. C., et al. (2005). Climatic influences on net ecosystem CO₂ exchange during the transition from wintertime carbon source to springtime carbon sink in a high-elevation, subalpine forest. *Oecologia*, 146(1), 130–147. https://doi.org/10.1007/s00442-005-0169-2
- Mote, P. W., Li, S., Lettenmaier, D. P., Xiao, M., & Engel, R. (2018). Dramatic declines in snowpack in the western US. Npj Climate and Atmospheric Science, 1(1), 1–6. https://doi.org/10.1038/s41612-018-0012-1
- Murray, M. B., Cannell, M. G. R., & Smith, R. I. (1989). Date of budburst of fifteen tree species in Britain following climatic warming. *Journal of Applied Ecology*, 26(2), 693–700. https://doi.org/10.2307/2404093
- Myneni, R. B., Keeling, C. D., Tucker, C. J., Asrar, G., & Nemani, R. R. (1997). Increased plant growth in the northern high latitudes from 1981 to 1991. Nature. 386(6626), 698–702. https://doi.org/10.1038/386698a0
- Nehemy, M. F., Maillet, J., Perron, N., Pappas, C., Sonnentag, O., Baltzer, J. L., et al. (2022). Snowmelt water use at transpiration onset: Phenology, isotope tracing, and tree water transit time. *Water Resources Research*, 58(9), e2022WR032344. https://doi.org/10.1029/2022WR032344
- Nehemy, M. F., Pierrat, Z., Maillet, J., Richardson, A. D., Stutz, J., Johnson, B., et al. (2023). Phenological assessment of transpiration: The stem-temp approach for determining start and end of season. *Agricultural and Forest Meteorology*, 331, 109319. https://doi.org/10.1016/j.agrformet. 2023.109319
- Noormets, A., Chen, J., Gu, L., & Desai, A. (2009). The phenology of gross ecosystem productivity and ecosystem respiration in temperate hardwood and conifer chronosequences. In A. Noormets (Ed.), *Phenology of ecosystem processes* (pp. 59–85). Springer. https://doi.org/10. 1007/978-1-4419-0026-5 3
- Pan, Y., Birdsey, R. A., Fang, J., Houghton, R., Kauppi, P. E., Kurz, W. A., et al. (2011). A large and persistent carbon sink in the world's forests. Science, 333(6045), 988–993. https://doi.org/10.1126/science.1201609
- Panwar, A., Migliavacca, M., Nelson, J. A., Cortés, J., Bastos, A., Forkel, M., & Winkler, A. J. (2023). Methodological challenges and new perspectives of shifting vegetation phenology in eddy covariance data. *Scientific Reports*, 13(1), 13885. https://doi.org/10.1038/s41598-023-41048-x
- Parazoo, N. C., Arneth, A., Pugh, T. A. M., Smith, B., Steiner, N., Luus, K., et al. (2018). Spring photosynthetic onset and net CO₂ uptake in Alaska triggered by landscape thawing. *Global Change Biology*, 24(8), 3416–3435. https://doi.org/10.1111/gcb.14283
- Peano, D., Hemming, D., Materia, S., Delire, C., Fan, Y., Joetzjer, E., et al. (2021). Plant phenology evaluation of CRESCENDO land surface models Part 1: Start and end of the growing season. *Biogeosciences*, 18(7), 2405–2428. https://doi.org/10.5194/bg-18-2405-2021
- Piao, S., Liu, Q., Chen, A., Janssens, I. A., Fu, Y., Dai, J., et al. (2019). Plant phenology and global climate change: Current progresses and challenges. *Global Change Biology*, 25(6), 1922–1940. https://doi.org/10.1111/gcb.14619
- Piao, S., Wang, X., Park, T., Chen, C., Lian, X., He, Y., et al. (2020). Characteristics, drivers and feedbacks of global greening. *Nature Reviews Earth & Environment*, *I*(1), 14–27. https://doi.org/10.1038/s43017-019-0001-x
- Piao, S., Wang, X., Wang, K., Li, X., Bastos, A., Canadell, J. G., et al. (2020). Interannual variation of terrestrial carbon cycle: Issues and perspectives. Global Change Biology, 26(1), 300–318. https://doi.org/10.1111/gcb.14884
- Pierrat, Z., Nehemy, M. F., Roy, A., Magney, T., Parazoo, N. C., Laroque, C., et al. (2021). Tower-based remote sensing reveals mechanisms behind a two-phased spring transition in a mixed-species boreal forest. *Journal of Geophysical Research: Biogeosciences*, 126(5), e2020JG006191. https://doi.org/10.1029/2020JG006191
- Pilegaard, K., & Ibrom, A. (2020). Net carbon ecosystem exchange during 24 years in the Sorø Beech Forest Relations to phenology and climate. Tellus B: Chemical and Physical Meteorology, 72(1), 1–17. https://doi.org/10.1080/16000889.2020.1822063

BOWLING ET AL. 22 of 25

21698961

- Post, A. K., Hufkens, K., & Richardson, A. D. (2022). Predicting spring green-up across diverse North American grasslands. *Agricultural and Forest Meteorology*, 327, 109204. https://doi.org/10.1016/j.agrformet.2022.109204
- Pulliainen, J., Aurela, M., Laurila, T., Aalto, T., Takala, M., Salminen, M., et al. (2017). Early snowmelt significantly enhances boreal springtime carbon uptake. *Proceedings of the National Academy of Sciences*, 114(42), 11081–11086. https://doi.org/10.1073/pnas.1707889114
- Richardson, A. D. (2019). Tracking seasonal rhythms of plants in diverse ecosystems with digital camera imagery. *New Phytologist*, 222(4), 1742–1750. https://doi.org/10.1111/nph.15591
- Richardson, A. D., Anderson, R. S., Arain, M. A., Barr, A. G., Bohrer, G., Chen, G., et al. (2012). Terrestrial biosphere models need better representation of vegetation phenology: Results from the north American carbon program site synthesis. *Global Change Biology*, 18(2), 566–584. https://doi.org/10.1111/j.1365-2486.2011.02562.x
- Richardson, A. D., Andy Black, T., Ciais, P., Delbart, N., Friedl, M. A., Gobron, N., et al. (2010). Influence of spring and autumn phenological transitions on forest ecosystem productivity. *Philosophical Transactions of the Royal Society B: Biological Sciences*, 365(1555), 3227–3246. https://doi.org/10.1098/rstb.2010.0102
- Richardson, A. D., Hollinger, D. Y., Dail, D. B., Lee, J. T., Munger, J. W., & O'keefe, J. (2009). Influence of spring phenology on seasonal and annual carbon balance in two contrasting New England forests. *Tree Physiology*, 29(3), 321–331. https://doi.org/10.1093/treephys/tpn040
- Richardson, A. D., Hufkens, K., Milliman, T., Aubrecht, D. M., Furze, M. E., Seyednasrollah, B., et al. (2018). Ecosystem warming extends vegetation activity but heightens vulnerability to cold temperatures. *Nature*, 560(7718), 368–371. https://doi.org/10.1038/s41586-018-0399-1
- Richardson, A. D., Keenan, T. F., Migliavacca, M., Ryu, Y., Sonnentag, O., & Toomey, M. (2013). Climate change, phenology, and phenological control of vegetation feedbacks to the climate system. *Agricultural and Forest Meteorology*, 169, 156–173. https://doi.org/10.1016/j.agrformet. 2012.09.012
- Schädel, C., Seyednasrollah, B., Hanson, P. J., Hufkens, K., Pearson, K. J., Warren, J. M., & Richardson, A. D. (2023). Using long-term data from a whole ecosystem warming experiment to identify best spring and autumn phenology models. *Plant-Environment Interactions*, 4(4), 188–200. https://doi.org/10.1002/pei3.10118
- Schulze, E. D., Fuchs, M., & Fuchs, M. I. (1977). Spacial distribution of photosynthetic capacity and performance in a mountain spruce forest of Northern Germany III. The Significance of the Evergreen Habit. *Oecologia*, 30(3), 239–248. https://doi.org/10.1007/BF01833630
- Schwartz, M. D., Ahas, R., & Aasa, A. (2006). Onset of spring starting earlier across the Northern Hemisphere. *Global Change Biology*, 12(2), 343–351. https://doi.org/10.1111/j.1365-2486.2005.01097.x
- Sen, P. K. (1968). Estimates of the regression coefficient based on Kendall's Tau. Journal of the American Statistical Association, 63(324), 1379–1389. https://doi.org/10.1080/01621459.1968.10480934
- Seneviratne, S. I., Corti, T., Davin, E. L., Hirschi, M., Jaeger, E. B., Lehner, I., et al. (2010). Investigating soil moisture–climate interactions in a changing climate: A review. *Earth-Science Reviews*, 99(3), 125–161. https://doi.org/10.1016/j.earscirev.2010.02.004
- Sevanto, S., Suni, T., Pumpanen, J., Grā¶nholm, T., Kolari, P., Nikinmaa, E., et al. (2006). Wintertime photosynthesis and water uptake in a
- boreal forest. Tree Physiology, 26(6), 749–757. https://doi.org/10.1093/treephys/26.6.749
 Siirila-Woodburn, E. R., Rhoades, A. M., Hatchett, B. J., Huning, L. S., Szinai, J., Tague, C., et al. (2021). A low-to-no snow future and its impacts
- Siirila-Woodburn, E. R., Rhoades, A. M., Hatchett, B. J., Huning, L. S., Szinai, J., Tague, C., et al. (2021). A low-to-no snow future and its impacts on water resources in the western United States. *Nature Reviews Earth & Environment*, 2(11), 800–819. https://doi.org/10.1038/s43017-021-00219-y
- Song, X., Wang, D.-Y., Li, F., & Zeng, X.-D. (2021). Evaluating the performance of CMIP6 Earth system models in simulating global vegetation structure and distribution. *Advances in Climate Change Research*, 12(4), 584–595. https://doi.org/10.1016/j.accre.2021.06.008
- Still, C., Powell, R., Aubrecht, D., Kim, Y., Helliker, B., Roberts, D., et al. (2019). Thermal imaging in plant and ecosystem ecology: Applications and challenges. *Ecosphere*, 10(6), e02768. https://doi.org/10.1002/ecs2.2768
- Tang, J., Körner, C., Muraoka, H., Piao, S., Shen, M., Thackeray, S. J., & Yang, X. (2016). Emerging opportunities and challenges in phenology: A review. *Ecosphere*, 7(8), e01436. https://doi.org/10.1002/ecs2.1436
- Tanja, S., Berninger, F., Vesala, T., Markkanen, T., Hari, P., Mäkelä, A., et al. (2003). Air temperature triggers the recovery of evergreen boreal forest photosynthesis in spring. *Global Change Biology*, 9(10), 1410–1426. https://doi.org/10.1046/j.1365-2486.2003.00597.x
- Teets, A., Bailey, A. S., Hufkens, K., Ollinger, S., Schädel, C., Seyednasrollah, B., & Richardson, A. D. (2023). Early spring onset increases carbon uptake more than late fall senescence: Modeling future phenological change in a US northern deciduous forest. *Oecologia*, 201(1), 241–257. https://doi.org/10.1007/s00442-022-05296-4
- Thornton, P. E., Shrestha, R., Thornton, M., Kao, S.-C., Wei, Y., & Wilson, B. E. (2021). Gridded daily weather data for North America with comprehensive uncertainty quantification. *Scientific Data*, 8(1), 190. https://doi.org/10.1038/s41597-021-00973-0
- Thum, T., Aalto, T., Laurila, T., Aurela, M., Hatakka, J., Lindroth, A., & Vesala, T. (2009). Spring initiation and autumn cessation of boreal coniferous forest CO₂ exchange assessed by meteorological and biological variables. *Tellus B: Chemical and Physical Meteorology*, 61(5), 701–717. https://doi.org/10.1111/j.1600-0889.2009.00441.x
- Turcotte, A., Morin, H., Krause, C., Deslauriers, A., & Thibeault-Martel, M. (2009). The timing of spring rehydration and its relation with the onset of wood formation in black spruce. *Agricultural and Forest Meteorology*, 149(9), 1403–1409. https://doi.org/10.1016/j.agrformet.2009. 03.010
- Vitasse, Y., Baumgarten, F., Zohner, C. M., Rutishauser, T., Pietragalla, B., Gehrig, R., et al. (2022). The great acceleration of plant phenological shifts. *Nature Climate Change*, 12(4), 300–302. https://doi.org/10.1038/s41558-022-01283-y
- Walther, S., Voigt, M., Thum, T., Gonsamo, A., Zhang, Y., Köhler, P., et al. (2016). Satellite chlorophyll fluorescence measurements reveal large-scale decoupling of photosynthesis and greenness dynamics in boreal evergreen forests. *Global Change Biology*, 22(9), 2979–2996. https://doi.org/10.1111/gcb.13200
- Wang, L., Lee, X., Wang, W., Wang, X., Wei, Z., Fu, C., et al. (2017). A meta-analysis of open-path eddy covariance observations of apparent CO2 flux in cold conditions in FLUXNET. *Journal of Atmospheric and Oceanic Technology*, 34(11), 2475–2487. https://doi.org/10.1175/ITFCH-D-17-0085.1
- Wang, X., Xiao, J., Li, X., Cheng, G., Ma, M., Zhu, G., et al. (2019). No trends in spring and autumn phenology during the global warming hiatus. Nature Communications, 10(1), 2389. https://doi.org/10.1038/s41467-019-10235-8
- Warm Winter 2020 Team, ICOS Ecosystem Thematic Centre. (2022). Warm winter 2020 ecosystem eddy covariance flux product for 73 stations in FLUXNET-archive format—Release 2022-1 (version 1.0) [Dataset]. ICOS Carbon Portal. https://doi.org/10.18160/2G60-ZHAK
- White, M. A., De Beurs, K. M., Didan, K., Inouye, D. W., Richardson, A. D., Jensen, O. P., et al. (2009). Intercomparison, interpretation, and assessment of spring phenology in North America estimated from remote sensing for 1982–2006. *Global Change Biology*, 15(10), 2335–2359. https://doi.org/10.1111/j.1365-2486.2009.01910.x
- Winchell, T. S., Barnard, D. M., Monson, R. K., Burns, S. P., & Molotch, N. P. (2016). Earlier snowmelt reduces atmospheric carbon uptake in midlatitude subalpine forests. *Geophysical Research Letters*, 43(15), 8168. https://doi.org/10.1002/2016GL069769

BOWLING ET AL. 23 of 25

- Wutzler, T., Lucas-Moffat, A., Migliavacca, M., Knauer, J., Sickel, K., Šigut, L., et al. (2018). Basic and extensible post-processing of eddy covariance flux data with REddyProc. *Biogeosciences*, 15(16), 5015–5030. https://doi.org/10.5194/bg-15-5015-2018
- Xia, J., Niu, S., Ciais, P., Janssens, I. A., Chen, J., Ammann, C., et al. (2015). Joint control of terrestrial gross primary productivity by plant phenology and physiology. In *Proceedings of the National Academy of Sciences*. 201413090. https://doi.org/10.1073/pnas.1413090112
- Xiang, Y., Gubian, S., Suomela, B., & Hoeng, J. (2013). The R journal: Generalized simulated annealing for global optimization: The GenSA package. The R Journal, 5(1), 13–28. https://doi.org/10.32614/RJ-2013-002
- Xin, Q., Broich, M., Zhu, P., & Gong, P. (2015). Modeling grassland spring onset across the Western United States using climate variables and MODIS-derived phenology metrics. Remote Sensing of Environment, 161, 63–77. https://doi.org/10.1016/j.rse.2015.02.003
- Xu, X., Du, H., Fan, W., Hu, J., Mao, F., & Dong, H. (2019). Long-term trend in vegetation gross primary production, phenology and their relationships inferred from the FLUXNET data. *Journal of Environmental Management*, 246, 605–616. https://doi.org/10.1016/j.jenvman. 2019.06.023
- Yang, L., & Noormets, A. (2021). Standardized flux seasonality metrics: A companion dataset for FLUXNET annual product. Earth System Science Data, 13(4), 1461–1475. https://doi.org/10.5194/essd-13-1461-2021
- Young-Robertson, J. M., Bolton, W. R., Bhatt, U. S., Cristóbal, J., & Thoman, R. (2016). Deciduous trees are a large and overlooked sink for snowmelt water in the boreal forest. Scientific Reports, 6(1), 29504. https://doi.org/10.1038/srep29504
- Zani, D., Crowther, T. W., Mo, L., Renner, S. S., & Zohner, C. M. (2020). Increased growing-season productivity drives earlier autumn leaf senescence in temperate trees. *Science*, 370(6520), 1066–1071. https://doi.org/10.1126/science.abd8911
- Zohner, C. M., Mirzagholi, L., Renner, S. S., Mo, L., Rebindaine, D., Bucher, R., et al. (2023). Effect of climate warming on the timing of autumn leaf senescence reverses after the summer solstice. *Science*, 381(6653), eadf5098. https://doi.org/10.1126/science.adf5098

References From the Supporting Information

- Amiro, B. D., Barr, A. G., Black, T. A., Iwashita, H., Kljun, N., McCaughey, J. H., et al. (2006). Carbon, energy and water fluxes at mature and disturbed forest sites, Saskatchewan, Canada. *Agricultural and Forest Meteorology*, 136(3), 237–251. https://doi.org/10.1016/j.agrformet. 2004.11.012
- Anderson-Teixeira, K. J., Delong, J. P., Fox, A. M., Brese, D. A., & Litvak, M. E. (2010). Differential responses of production and respiration to temperature and moisture drive the carbon balance across a climatic gradient in New Mexico. *Global Change Biology*, 17(1), 410–424. https://doi.org/10.1111/j.1365-2486.2010.02269.x
- Anthoni, P. M., Knohl, A., Rebmann, C., Freibauer, A., Mund, M., Ziegler, W., et al. (2004). Forest and agricultural land-use-dependent CO₂ exchange in Thuringia, Germany. *Global Change Biology*, 10(12), 2005–2019. https://doi.org/10.1111/j.1365-2486.2004.00863.x
- Arain, M. A., Xu, B., Brodeur, J. J., Khomik, M., Peichl, M., Beamesderfer, E., et al. (2022). Heat and drought impact on carbon exchange in an age-sequence of temperate pine forests. *Ecological Processes*, 11(1), 7. https://doi.org/10.1186/s13717-021-00349-7
- Brown, M., Black, T. A., Nesic, Z., Foord, V. N., Spittlehouse, D. L., Fredeen, A. L., et al. (2010). Impact of mountain pine beetle on the net ecosystem production of lodgepole pine stands in British Columbia. *Agricultural and Forest Meteorology*, 150(2), 254–264. https://doi.org/10.1016/j.agrformet.2009.11.008
- Burns, S. P., Blanken, P. D., Turnipseed, A. A., Hu, J., & Monson, R. K. (2015). The influence of warm-season precipitation on the diel cycle of the surface energy balance and carbon dioxide at a Colorado subalpine forest site. *Biogeosciences*, 12(23), 7349–7377. https://doi.org/10.5194/bp-12-7349-7015
- Coursolle, C., Margolis, H. A., Barr, A. G., Black, T. A., Amiro, B. D., McCaughey, J. H., et al. (2006). Late-summer carbon fluxes from Canadian forests and peatlands along an east-west continental transect. *Canadian Journal of Forest Research*, 36(3), 783–800. https://doi.org/10.1139/x05-270
- Desai, A. R., Bolstad, P. V., Cook, B. D., Davis, K. J., & Carey, E. V. (2005). Comparing net ecosystem exchange of carbon dioxide between an old-growth and mature forest in the upper Midwest, USA. *Agricultural and Forest Meteorology*, 128(1), 33–55. https://doi.org/10.1016/j.agrformet.2004.09.005
- Desai, A. R., Helliker, B. R., Moorcroft, P. R., Andrews, A. E., & Berry, J. A. (2010). Climatic controls of interannual variability in regional carbon fluxes from top-down and bottom-up perspectives. *Journal of Geophysical Research*, 115(G2). https://doi.org/10.1029/2009JG001122
- Dunn, A. L., Barford, C. C., Wofsy, S. C., Goulden, M. L., & Daube, B. C. (2007). A long-term record of carbon exchange in a boreal black spruce forest: Means, responses to interannual variability, and decadal trends. *Global Change Biology*, 13(3), 577–590. https://doi.org/10.1111/j.1365-2486.2006.01221.x
- Frank, J. M., Massman, W. J., Ewers, B. E., Huckaby, L. S., & Negrón, J. F. (2014). Ecosystem CO₂/H₂O fluxes are explained by hydraulically limited gas exchange during tree mortality from spruce bark beetles. *Journal of Geophysical Research: Biogeosciences*, 119(6), 1195–1215. https://doi.org/10.1002/2013JG002597
- Gough, C. M., Vogel, C. S., Schmid, H. P., Su, H.-B., & Curtis, P. S. (2008). Multi-year convergence of biometric and meteorological estimates of forest carbon storage. Agricultural and Forest Meteorology, 148(2), 158–170. https://doi.org/10.1016/j.agrformet.2007.08.004
- Griffis, T. J., Black, T. A., Morgenstern, K., Barr, A. G., Nesic, Z., Drewitt, G. B., et al. (2003). Ecophysiological controls on the carbon balances of three southern boreal forests. Agricultural and Forest Meteorology, 117(1), 53–71. https://doi.org/10.1016/S0168-1923(03)00023-6
- Jocher, G., Fischer, M., Šigut, L., Pavelka, M., Sedlák, P., & Katul, G. (2020). Assessing decoupling of above and below canopy air masses at a Norway spruce stand in complex terrain. Agricultural and Forest Meteorology, 294, 108149. https://doi.org/10.1016/j.agrformet.2020.108149
- Knohl, A., Schulze, E.-D., Kolle, O., & Buchmann, N. (2003). Large carbon uptake by an unmanaged 250-year-old deciduous forest in Central Germany. Agricultural and Forest Meteorology, 118(3), 151–167. https://doi.org/10.1016/S0168-1923(03)00115-1
- Korkiakoski, M., Ojanen, P., Tuovinen, J.-P., Minkkinen, K., Nevalainen, O., Penttilä, T., et al. (2023). Partial cutting of a boreal nutrient-rich peatland forest causes radically less short-term on-site CO₂ emissions than clear-cutting. *Agricultural and Forest Meteorology*, 332, 109361. https://doi.org/10.1016/j.agrformet.2023.109361
- Kurbatova, J., Li, C., Varlagin, A., Xiao, X., & Vygodskaya, N. (2008). Modeling carbon dynamics in two adjacent spruce forests with different soil conditions in Russia. *Biogeosciences*, 5(4), 969–980. https://doi.org/10.5194/bg-5-969-2008
- Lagergren, F., Lindroth, A., Dellwik, E., Ibrom, A., Lankreijer, H., Launiainen, S., et al. (2008). Biophysical controls on CO₂ fluxes of three Northern forests based on long-term eddy covariance data. *Tellus Series B Chemical and Physical Meteorology*, 60(2), 143–152. https://doi.org/10.1111/j.1600-0889.2006.00324.x
- Lasslop, G., Reichstein, M., Papale, D., Richardson, A. D., Arneth, A., Barr, A., et al. (2010). Separation of net ecosystem exchange into assimilation and respiration using a light response curve approach: Critical issues and global evaluation. Global Change Biology, 16(1), 187–208. https://doi.org/10.1111/j.1365-2486.2009.02041.x

BOWLING ET AL. 24 of 25



Journal of Geophysical Research: Biogeosciences

- 10.1029/2023JG007839
- Lee, X., Fuentes, J. D., Staebler, R. M., & Neumann, H. H. (1999). Long-term observation of the atmospheric exchange of CO₂ with a temperate deciduous forest in southern Ontario, Canada. *Journal of Geophysical Research*, 104(D13), 15975–15984. https://doi.org/10.1029/1999ID900227
- Lindauer, M., Schmid, H. P., Grote, R., Mauder, M., Steinbrecher, R., & Wolpert, B. (2014). Net ecosystem exchange over a non-cleared wind-throw-disturbed upland spruce forest—Measurements and simulations. Agricultural and Forest Meteorology, 197, 219–234. https://doi.org/10.1016/j.agrformet.2014.07.005
- Litvak, M., Miller, S., Wofsy, S. C., & Goulden, M. (2003). Effect of stand age on whole ecosystem CO2 exchange in the Canadian boreal forest. *Journal of Geophysical Research*, 108(D3). https://doi.org/10.1029/2001JD000854
- Martel, M.-C., Margolis, H. A., Coursolle, C., Bigras, F. J., Heinsch, F. A., & Running, S. W. (2005). Decreasing photosynthesis at different spatial scales during the late growing season on a boreal cutover. *Tree Physiology*, 25(6), 689–699. https://doi.org/10.1093/treephys/25.6.689
- Mkhabela, M. S., Amiro, B. D., Barr, A. G., Black, T. A., Hawthorne, I., Kidston, J., et al. (2009). Comparison of carbon dynamics and water use efficiency following fire and harvesting in Canadian boreal forests. *Agricultural and Forest Meteorology*, 149(5), 783–794. https://doi.org/10.1016/j.agrformet.2008.10.025
- Montagnani, L., Manca, G., Canepa, E., Georgieva, E., Acosta, M., Feigenwinter, C., et al. (2009). A new mass conservation approach to the study of CO₂ advection in an alpine forest. *Journal of Geophysical Research*, 114(D7). https://doi.org/10.1029/2008JD010650
- Nagano, H., Ikawa, H., Nakai, T., Matsushima-Yashima, M., Kobayashi, H., Kim, Y., & Suzuki, R. (2018). Extremely dry environment down-regulates nighttime respiration of a black spruce forest in Interior Alaska. Agricultural and Forest Meteorology, 249, 297–309. https://doi.org/10.1016/j.agrformet.2017.11.001
- Nave, L. E., Gough, C. M., Maurer, K. D., Bohrer, G., Hardiman, B. S., Le Moine, J., et al. (2011). Disturbance and the resilience of coupled carbon and nitrogen cycling in a north temperate forest. *Journal of Geophysical Research*, 116(G4), G04016. https://doi.org/10.1029/2011JG001758
- Ovaskainen, O., Meyke, E., Lo, C., Tikhonov, G., Delgado, M. D. M., Roslin, T., et al. (2020). Chronicles of nature calendar, a long-term and large-scale multitaxon database on phenology. *Scientific Data*, 7(1), 47. https://doi.org/10.1038/s41597-020-0376-z
- Pastorello, G., Trotta, C., Canfora, E., Chu, H., Christianson, D., Cheah, Y.-W., et al. (2020). The FLUXNET2015 dataset and the ONEFlux processing pipeline for eddy covariance data. *Scientific Data*, 7(1), 225. https://doi.org/10.1038/s41597-020-0534-3
- Pluntke, T., Bernhofer, C., Grünwald, T., Renner, M., & Prasse, H. (2023). Long-term climatological and ecohydrological analysis of a paired catchment Flux tower observatory near Dresden (Germany). Is there evidence of climate change in local evapotranspiration? *Journal of Hydrology*, 617, 128873. https://doi.org/10.1016/j.jhydrol.2022.128873
- Reichstein, M., Falge, E., Baldocchi, D., Papale, D., Aubinet, M., Berbigier, P., et al. (2005). On the separation of net ecosystem exchange into assimilation and ecosystem respiration: Review and improved algorithm. *Global Change Biology*, 11(9), 1424–1439. https://doi.org/10.1111/j. 1365-2486.2005.001002.x
- Richardson, A. D., Jenkins, J. P., Braswell, B. H., Hollinger, D. Y., Ollinger, S. V., & Smith, M.-L. (2007). Use of digital webcam images to track spring green-up in a deciduous broadleaf forest. *Oecologia*, 152(2), 323–334. https://doi.org/10.1007/s00442-006-0657-z
- Thomas, V., Finch, D. A., McCaughey, J. H., Noland, T., Rich, L., & Treitz, P. (2006). Spatial modelling of the fraction of photosynthetically active radiation absorbed by a boreal mixedwood forest using a lidar–hyperspectral approach. *Agricultural and Forest Meteorology*, 140(1), 287–307. https://doi.org/10.1016/j.agrformet.2006.04.008
- Ueyama, M., Iwata, H., & Harazono, Y. (2014). Autumn warming reduces the CO₂ sink of a black spruce forest in interior Alaska based on a nineyear eddy covariance measurement. Global Change Biology, 20(4), 1161–1173. https://doi.org/10.1111/gcb.12434
- Valentini, R., De Angelis, P., Matteucci, G., Monaco, R., Dore, S., & Mucnozza, G. E. S. (1996). Seasonal net carbon dioxide exchange of a beech forest with the atmosphere. *Global Change Biology*, 2(3), 199–207. https://doi.org/10.1111/j.1365-2486.1996.tb00072.x

BOWLING ET AL. 25 of 25